Supplementary Information

Hydrogen Phosphates Play a Critical Structural Role in Amorphous Calcium Phosphates

Shu-Li Li,[1a] Li-Han Wang,[1a] Yi-Tan Lin,[a] Shing-Jong Huang,[b] Jerry C. C. Chan*[a]

[a] Department of Chemistry, National Taiwan University, No. 1, Section 4, Roosevelt Road, Taipei, 10617, Taiwan.

[b] Instrumentation Center, National Taiwan University, No. 1, Section 4, Roosevelt Road, Taipei, 10617, Taiwan.

[1] These authors contributed equally to this work.

* To whom correspondence should be addressed, e-mail: chanjcc@ntu.edu.tw

Table of Contents

1. Materials and Methods

Sample Preparation. All chemicals were obtained from Acros unless stated otherwise. The $ACP_{9.7}$ sample was prepared by mixing the solutions of 250 mM of $Ca(NO_3)_{2(aq)}$ and 150 mM of $(NH_4)_2HPO_{4(aq)}$ at pH 10.0 in a micromixer of volume 1.2 μL (YMC, YSP 101) at 1 °C. The final pH after the precipitation was 9.70. The reaction was quenched in precooled acetone. After several cycles of centrifugation-wash by ethanol and deionized water, the sample was lyophilized. The ACHP sample was prepared by mixing 3 mL of $CaCl_{2(aq)}$ (557 mM) and 3 mL of of $Na_2HPO_{4(aq)}$ (333 mM, pH 9.0). To the solution mixture with white precipitate formed immediately, 40 mL of methanol was added. The precipitate was collected by centrifugation and repeat washing with methanol and acetone. For the preparation of ACP through the non-aqueous route, we followed the protocol developed by Tang and co-workers.[1] Briefly, 0.22 g of $CaCl_2 \cdot 2H_2O$ was dissolved in 60 mL of ethanol (25 mM), to which 40 mL of an ethanol solution of H_3PO_4 (25 mM) and triethylamine (750 mM) were added under ambient conditions. After stirring for 30 min, the gel-like sample was collected by two rounds of centrifugation (12000*g* for 20 min) and resuspension in ethanol. The sample was dried under reduced pressure (0.03 to 0.04 MPa) with silica gel desiccant for 3 days. For the preparation of CaP-PAA, a solution mixture of NaH_2PO_4 (500 mM) and polyacrylic acid (PAA, MW = 2000, 4.5 mM) was adjusted to pH 6.0. To 5 mL of the mixture an aqueous solution of 5 mL of $CaCl_2$ (100 mM) was added under ambient conditions. After setting for 24 hours at 37 °C, the final pH was 5.61 and the sample was collected by two rounds of centrifugation (12000*g* for 10 min) and resuspension in deionized (DI) water. The samples were subsequently dried by lyophilization or under reduced pressure (0.005 MPa).

Sample Characterization. Scanning electron microscopy (SEM) images and energy dispersive X-ray (EDX) analyses were taken on JEOL JSM-7600F field emission scanning electron microscope equipped with EDX accessories. Infrared spectra were acquired on a Spectrum Two FT-IR Spectrometer (PerkinElmer) with the accessory of attenuated total reflectance (MIRacle, PIKE Technologies). X-ray powder diffraction (XRD) analyses were performed on a Bruker D2 Phaser diffractometer using Cu-K_α radiation (λ = 1.5418 Å). For the thermogravimetric analysis (TGA), the samples were heated in Mettler

DSC/TGA 1 from 40 to 800 °C at a ramping rate of 10 °C/min with air purging (50 mL/min). Optical microscopy (OM) images were taken on Olympus BX53 equipped with Olympus E-M5II camera. Transmission Electron Microscopy (TEM) imaging and TEM-EDX mapping were carried out on a JEOL JEM-2100F field emission gun transmission microscope equipped with EDX accessories (OXFORD X-MaxN TSR EDX) at an operating voltage of 200 kV.

Solid state NMR. $^{31}P\{^{1}H\}$ heteronuclear correlation (HETCOR) spectra were acquired at 9.4 T (^{31}P and ^{1}H Larmor frequencies of 161.98 and 400.15 MHz, respectively) on Bruker Avance III spectrometers equipped with a commercial 2.5 mm probe. The sample spectra were acquired at the spinning frequencies of 10 and 20 kHz. The cross-polarization (CP) contact time was set to 2 ms, unless stated otherwise. During the CP period, the ^{31}P nutation frequency were set to 34.5 and 70.7 kHz at the spinning frequencies of 10 and 20 kHz, respectively, and that of ^{1}H was linearly ramped from 40.7 to 50.9 kHz to fulfill the Hartmann-Hahn matching condition. For each t_1 increment, 32 transients were accumulated and a total of 200 increments were acquired at steps of 10 μs. For selected samples, the t_1 increment was rotor synchronized. ^{31}P and ^{1}H chemical shifts were externally referenced to 85% phosphoric acid and tetramethylsilane, respectively, using commercial HAp (Sigma-Aldrich) as the secondary reference, for which the ^{31}P and ^{1}H chemical shifts of the HAp were set to 2.8 and 0.2 ppm, respectively.

2. Results and Discussion

Solid-State NMR Characterization of the ACP Model Compounds. The samples of $ACP_{9.7}$ and ACHP were characterized by their IR spectra (Fig. S1). Fig. S2 shows the solid-state $^{31}P\{^{1}H\}$ heteronuclear correlation (HETCOR) spectrum of ACHP, which was dominated by the correlation peak at 13.2 ppm (^{1}H) and 0.7 ppm (^{31}P). The chemical shifts are consistent with the literature data reported for hydrogen phosphate (HPO_4^{2-}).[2] For the $ACP_{9.7}$ spectrum, there were two spectral components. The ^{31}P peaks at 2.3 and 2.0 ppm were correlated to the ^{1}H peaks at 6.8 and 13.5 ppm, respectively. The former of the two ^{1}H peaks could be readily assigned to structural water and the latter to the acidic proton of hydrogen phosphate. As shown in the full ^{1}H projection spectra (Fig. S2), the water signal of $ACP_{9.7}$ had substantial spinning sidebands, whereas the spinning sidebands of hydrogen phosphate was much less pronounced for ACHP. This observation is consistent with the fact that the intramolecular ^{1}H homonuclear dipolar interaction between the two ^{1}H spins of water are significantly stronger than the corresponding intermolecular interaction among the ^{1}H spins of hydrogen phosphate ions. Note that the spinning sidebands of the water signal would be substantially attenuated if significant motional dynamics of the water molecules occur. For both the ACHP and $ACP_{9.7}$ samples, the full width at half maximum (FWHM) of the ^{31}P and ^{1}H signals were > 5 ppm.

The ^{31}P chemical shifts of hydrogen phosphate are usually less than 1 ppm for CaP systems,[2] which are more shielded ("up-field") than what we observed for $ACP_{9.7}$ (2.0 ppm). To clarify this issue, we measured a series of $^{31}P\{^{1}H\}$ HETCOR spectra with variable contact time, from which the signal intensities $M(t)$ as a function of the contact time *t* were analyzed by the following equation:

$$M(t) = M_0(1 - e^{\frac{-t}{\tau_{CP}}})e^{\frac{-t}{T_{1\rho}}} \qquad \text{(S1)}$$

where τ_{CP} denotes the exponential signal build-up rate and $T_{1\rho}$ the decay rate of the spin-locked ^{1}H magnetization. The value of τ_{CP}, which characterizes the rate of polarization transfer between the ^{1}H and ^{31}P species, could be correlated to the bond distance between the acidic proton and the phosphorous nucleus of $H—OPO_3^{2-}$. For

this experiment, we used monetite ($CaHPO_4$) as a reference compound for hydrogen phosphate (Figs. S3–S7).[3] The results are summarized in Table S1. For ACHP shown in Fig. S8, the τ_{CP} obtained for the correlation peak between the ^1H signal at 13.2 ppm and the ^{31}P signal at 0.7 ppm, i.e., τ_{CP}(ACHP, 13.2 ppm, 0.7 ppm), was found to be 0.38 ± 0.03 ms, which is almost the same as the τ_{CP} obtained for the hydrogen phosphate of monetite. Interestingly, we have τ_{CP}($ACP_{9.7}$, 13.5 ppm, 2.0 ppm) equal to 0.56 ± 0.03 ms. This somewhat larger τ_{CP} value is not likely due to the attenuation of the polarization transfer rate by the molecular tumbling of hydrogen phosphate, because of the intense spinning sidebands of the water signal (Fig. S2). Yet, there are two plausible scenarios. First, the proton of the hydrogen phosphate in $ACP_{9.7}$ may undergo hopping between the phosphate ions and the coupled water network. Alternatively, the hydrogen phosphate might have formed hydrogen bond with the neighboring water, i.e., $H_2O \cdots HOPO_3^{2-}$. Both scenarios would lead to a lengthening of the distance between ^1H and ^{31}P, rendering a longer τ_{CP} than that of an isolated and static HPO_4^{2-} . On the other hand, τ_{CP}($ACP_{9.7}$, 6.8 ppm, 2.3 ppm) was 0.97 ± 0.07 ms, which was taken as a reference value for the scenario of orthophosphate ions in close proximity to water.

3. Figures

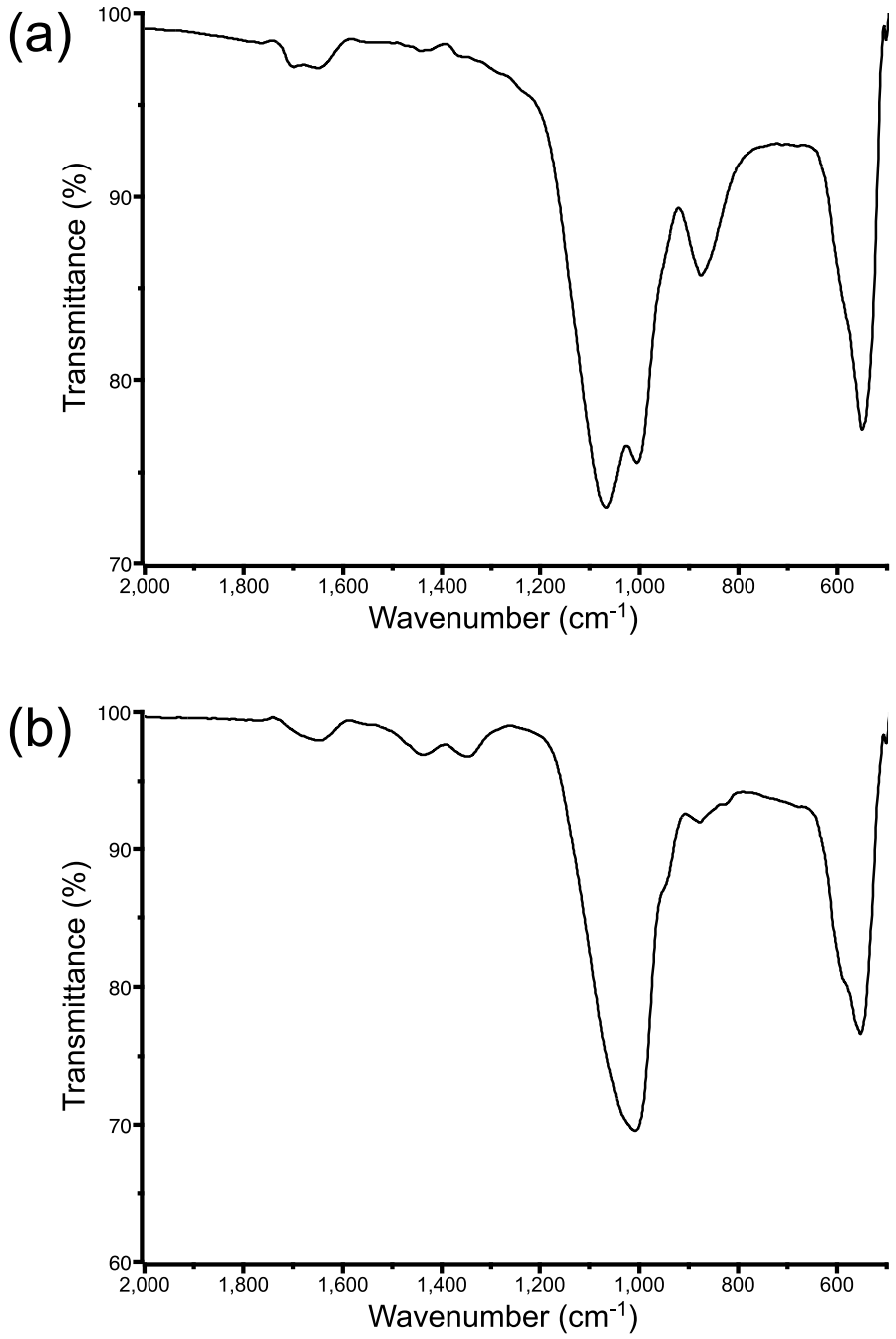

Figure S1. FT-IR spectra of (a) ACHP (b) $ACP_{9.7}$.

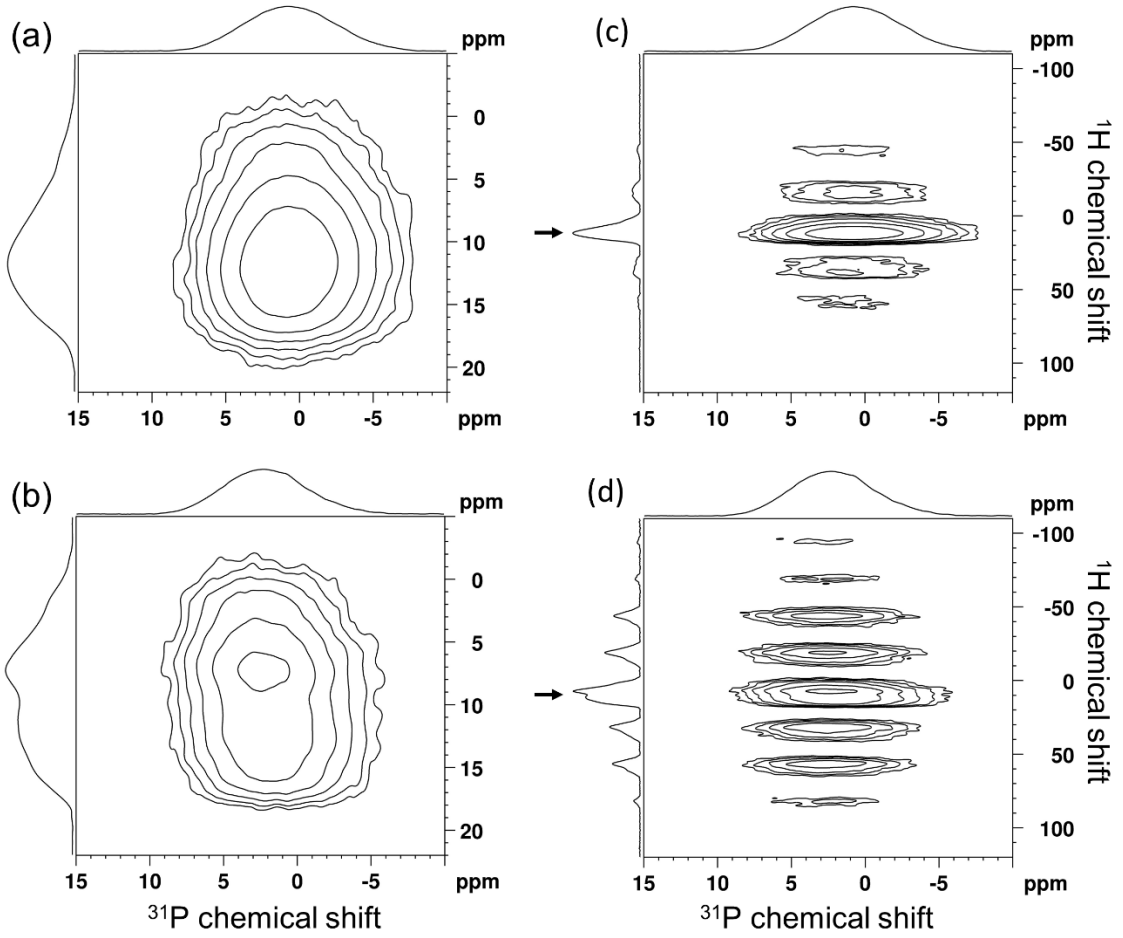

Figure S2. $^{31}P\{^{1}H\}$ HECTCOR spectra acquired for (a) ACHP and (b) $ACP_{9.7}$ at a contact time of 2 ms. The spectra including the full sideband manifold in the ^{1}H dimension are shown in (c) ACHP and (d) $ACP_{9.7}$, where the arrows indicate the positions of the center bands and other peaks are spinning sidebands. The contour levels were increased by a factor of 1.8 successively, where the base level was set to 5 × root-mean-square noise

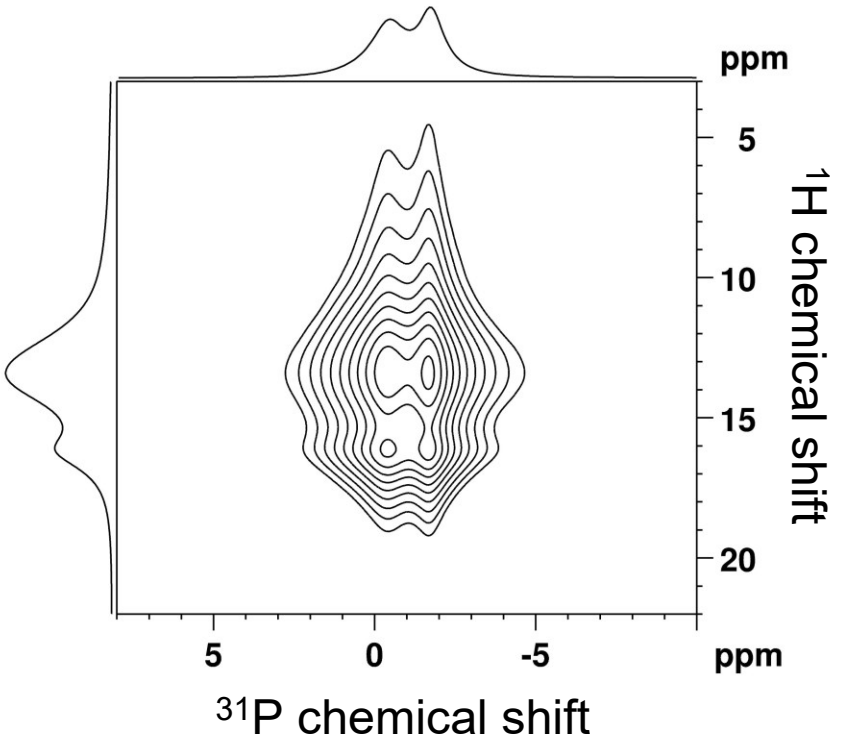

Figure S3. $^{31}P\{^{1}H\}$ HETCOR spectra acquired for monetite sample at a contact time of 2 ms. The contour levels were increased by a factor of 1.4 successively, where the base level was set to 100 × root-mean-square noise. By spectral deconvolution, the intensity modulation of the four correlation peaks as a function of the contact time was monitored.

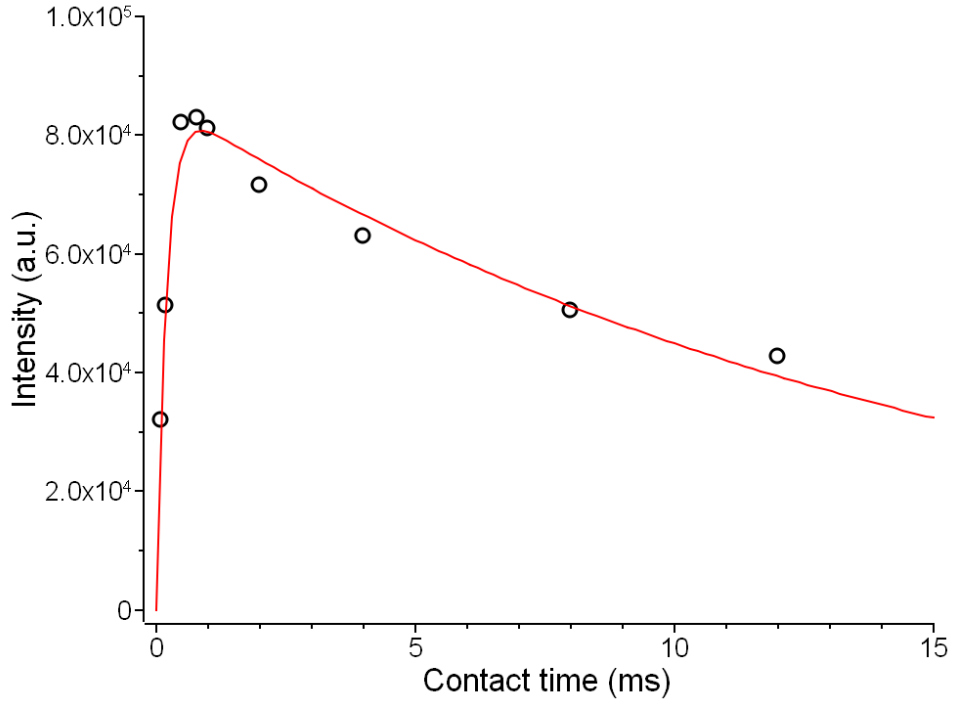

Figure S4. Fitting of the intensity modulation of the correlation peak at (^{1}H: 16.3 ppm, ^{31}P: –0.4 ppm) of the monetite by the equation S1. The correlation peak corresponded to the ^{1}H to ^{31}P polarization transfer within the hydrogen phosphate ion of $\mathrm{H1P2O_4^{2-}}$, where the label of the hydrogen and phosphorus atoms follow the assignment suggested in the literature.[3] The green and red colors denote the source and the detected nuclei. The extracted τ_{CP} and $T_{1\rho}$ were 0.20 ± 0.02 and 15 ± 2 ms, respectively.

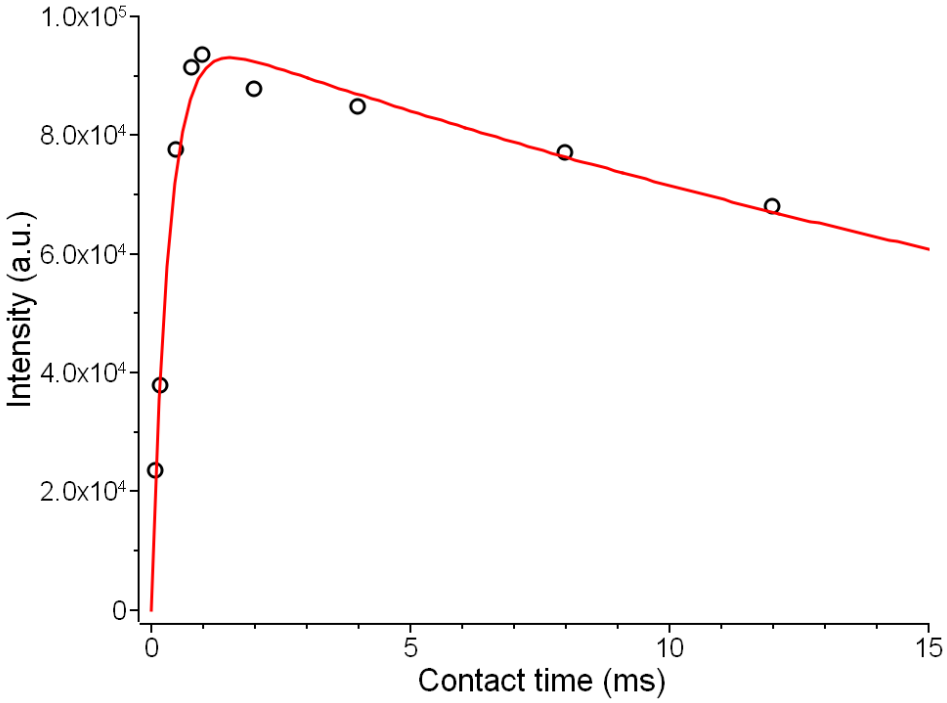

Figure S5. Fitting of the intensity modulation of the correlation peak at (^{1}H: 13.5 ppm, ^{31}P: −1.7 ppm) of the monetite by the equation S1. The correlation peak corresponded to the ^{1}H to ^{31}P polarization transfer within the hydrogen phosphate ion of H2P1O_4^{2-}. The extracted τ_{CP} and $T_{1\rho}$ were 0.34 ± 0.04 and 31 ± 6 ms, respectively. See also the caption of **Figure S4**.

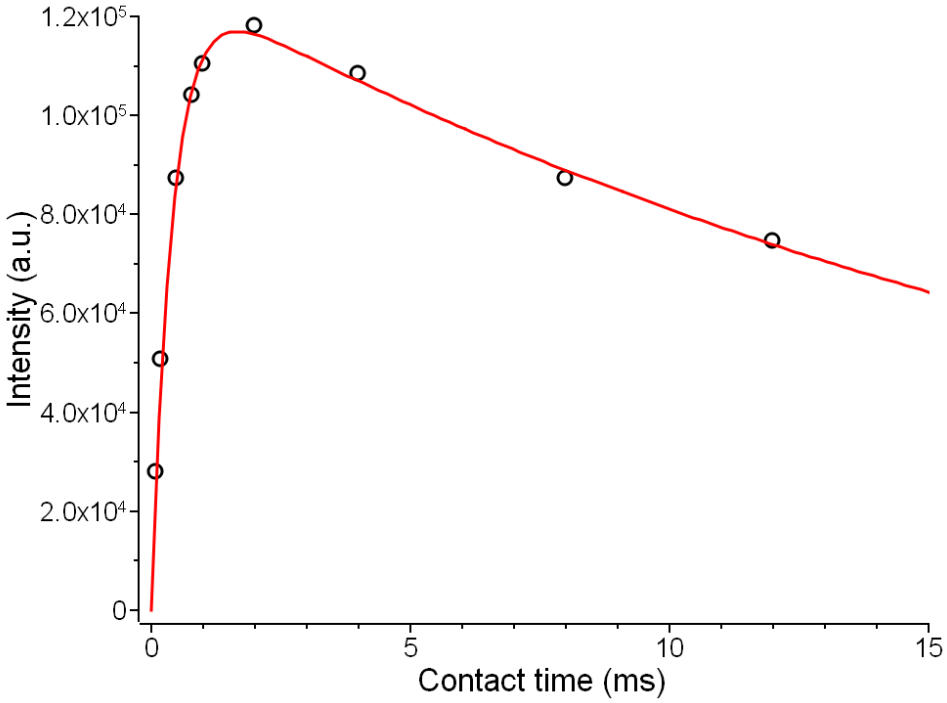

Figure S6. Fitting of the intensity modulation of the correlation peak at (^{1}H: 13.5 ppm, ^{31}P: –0.4 ppm) of the monetite by the equation S1. The correlation peak corresponded to the intermolecular ^{1}H to ^{31}P polarization transfer between two hydrogen-bonded hydrogen phosphate ions, viz., $\mathrm{H2PO_4^{2-}} \cdots \mathrm{HP2O_4^{2-}}$. The extracted τ_{CP} and $T_{1\rho}$ were 0.42 ± 0.02 and 22 ± 1 ms, respectively. See also the caption of **Figure S4.**

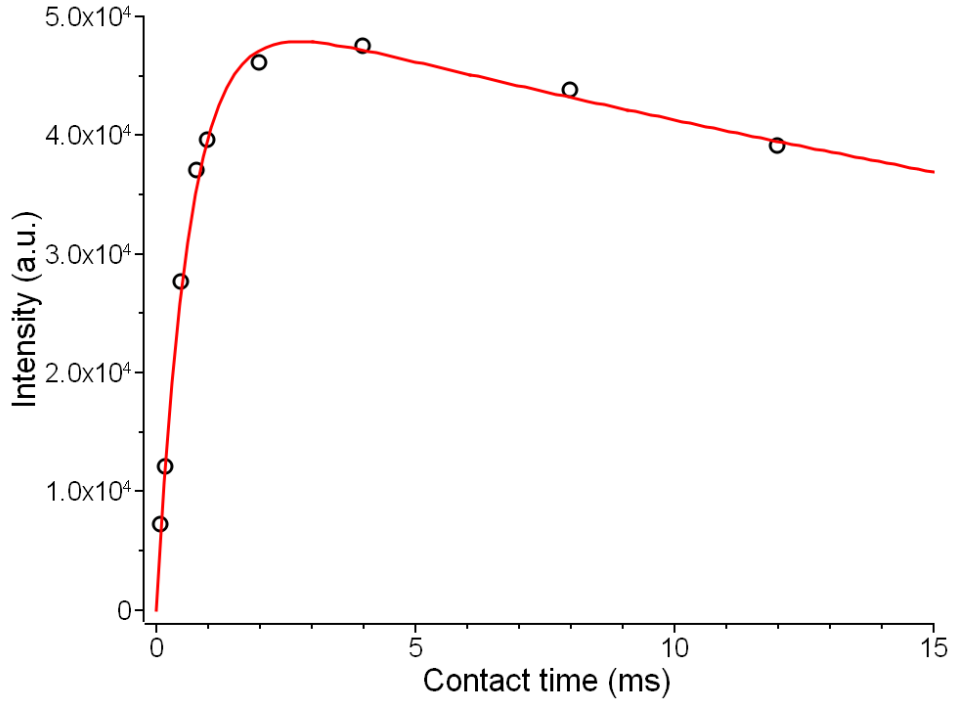

Figure S7. Fitting of the intensity modulation of the correlation peak at (^{1}H: 16.3 ppm, ^{31}P: −1.7 ppm) of the monetite by the equation S1. The correlation peak corresponded to the intermolecular ^{1}H to ^{31}P polarization transfer between two neighboring hydrogen phosphate ions, viz., $\mathrm{H1PO_4^{2-}/HP1O_4^{2-}}$. The extracted τ_{CP} and $T_{1\rho}$ were 0.65 ± 0.03 and 44 ± 6 ms, respectively. See also the caption of **Figure S4**.

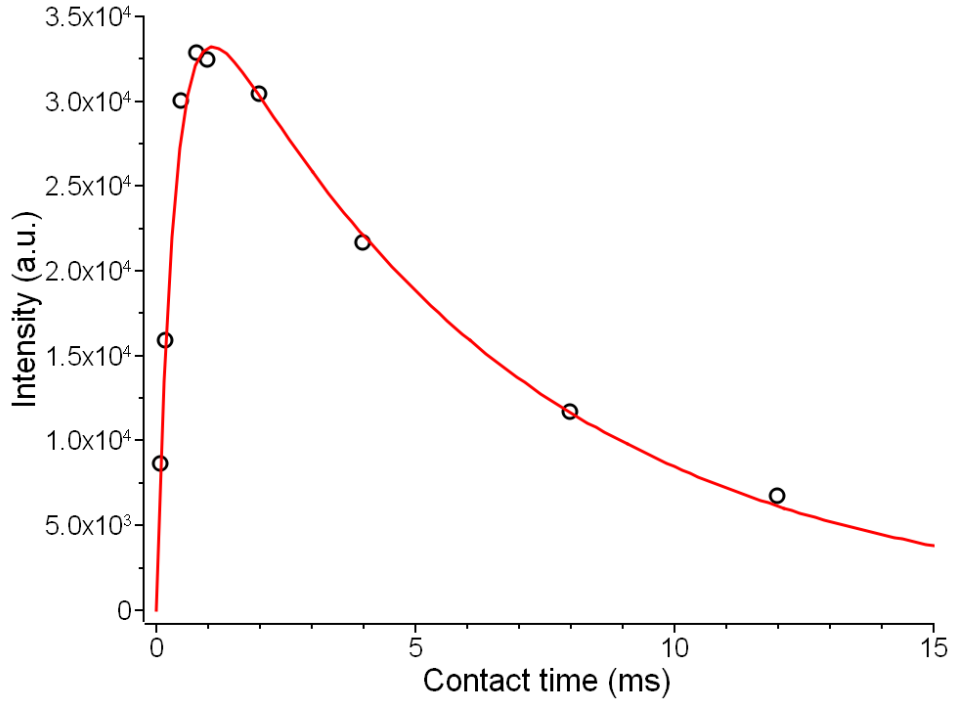

Figure S8. Fitting of the intensity modulation of the correlation peak at (^{1}H: 13.2 ppm, ^{31}P: 0.7 ppm) of the ACHP by the equation S1. The correlation peak corresponded to the ^{1}H to ^{31}P polarization transfer within the hydrogen phosphate ion of HPO_4^{2-}. The extracted τ_{CP} and $T_{1\rho}$ were 0.38 ± 0.03 and 6.2 ± 0.4 ms, respectively. See the caption of **Figure S4** for the color code.

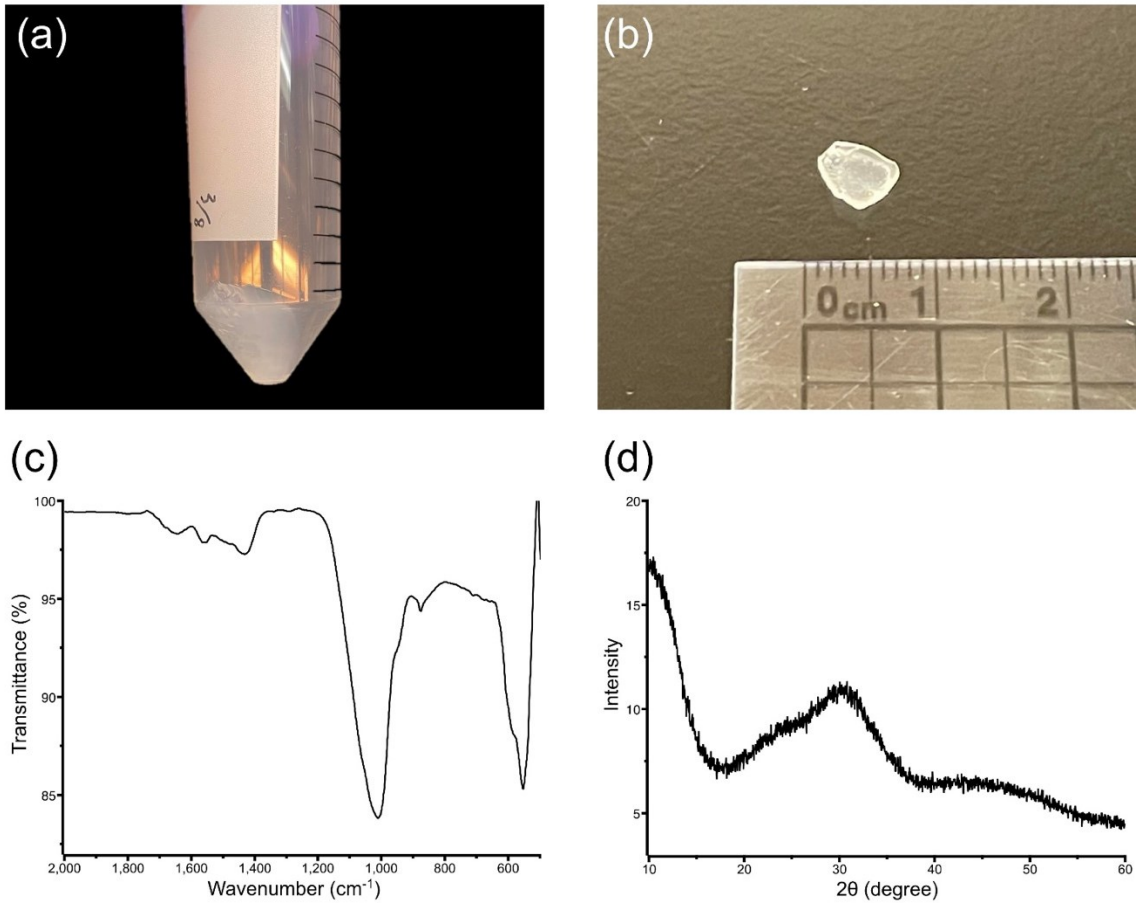

Figure S9. (a) Photo of the gel-like ACP_{TEA} before drying. (b) Photo of ACP_{TEA} after drying under reduced pressure. (c) FT-IR spectrum of ACP_{TEA}. (d) XRD pattern of ACP_{TEA}.

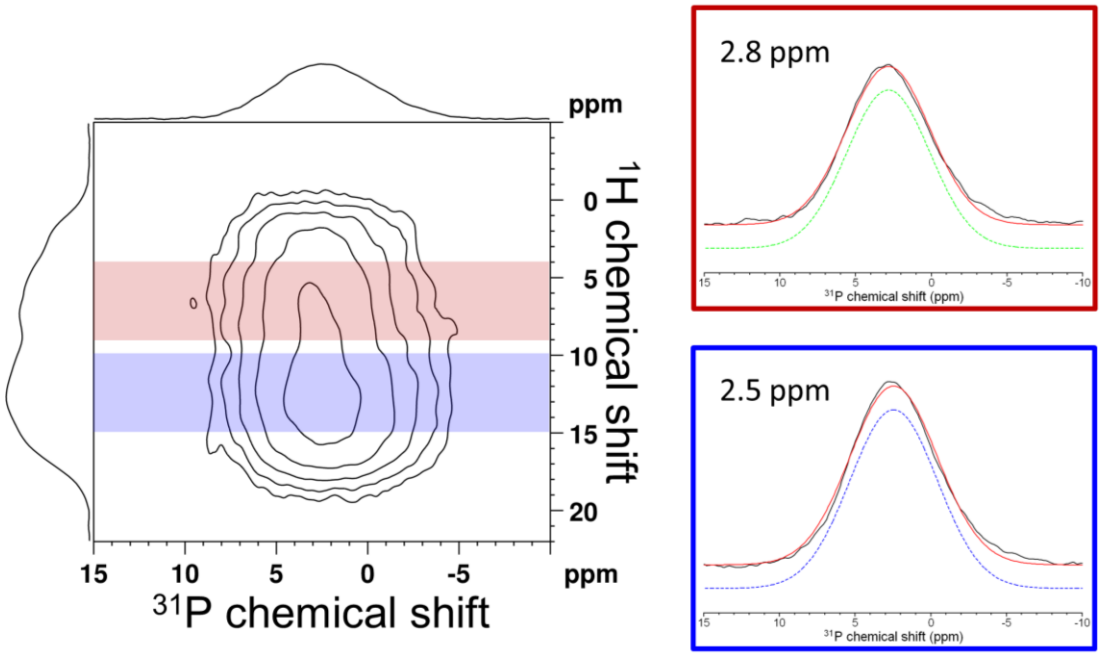

Figure S10. ^{31}P{^{1}H} HETCOR spectrum acquired for ACP_{TEA}. The ^{31}P projections along the shaded regions of the ^{1}H dimension from 4 to 9 and 10 to 15 ppm are shown on the right, on which the ^{31}P chemical shifts determined by spectral deconvolution are provided. The color code of the box boundaries is matched to that of the shaded regions.

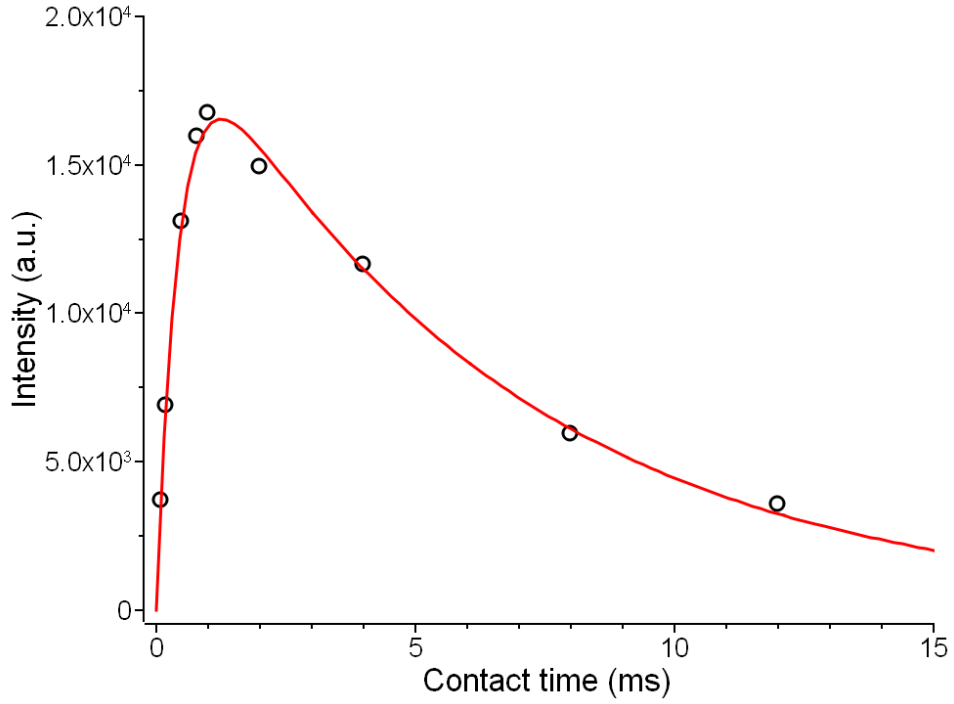

Figure S11. Fitting of the intensity modulation of the correlation peak at (^{1}H: 6.6 ppm, ^{31}P: 2.8 ppm) of ACP_{TEA} by the equation S1. The correlation peak corresponded to the ^{1}H to ^{31}P polarization transfer of $HOH\cdots OPO_3^{3-}$. The extracted τ_{CP} and $T_{1\rho}$ were 0.47 ± 0.04 and 6.3 ± 0.4 ms, respectively. See the caption of **Figure S4** for the color code.

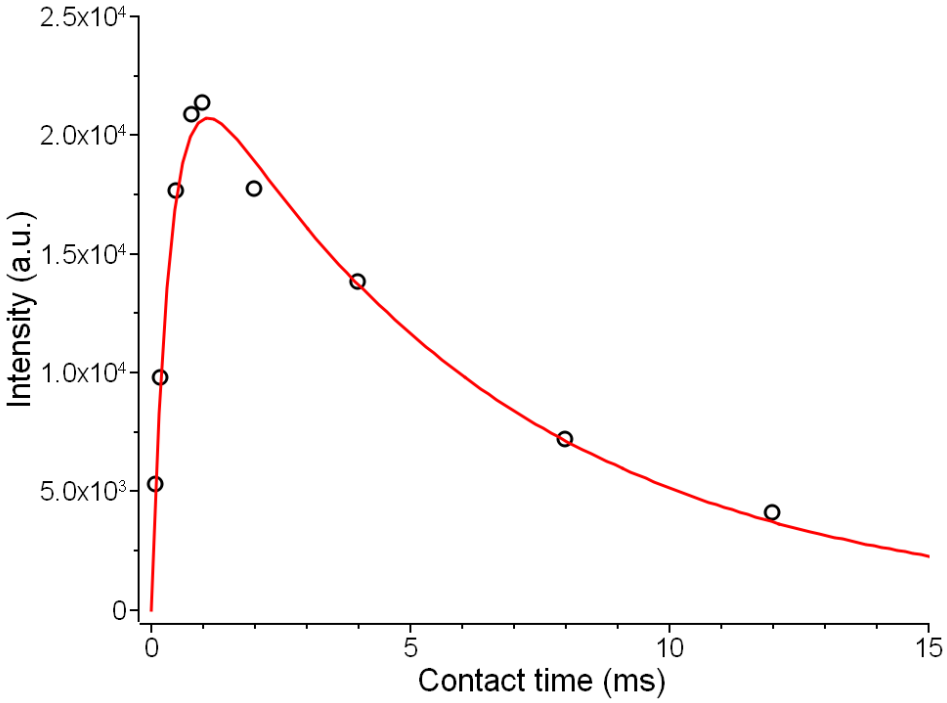

Figure S12. Fitting of the intensity modulation of the correlation peak at (^{1}H: 13.7 ppm, ^{31}P: 2.5 ppm) of ACP_{TEA} by the equation S1. The correlation peak corresponded to the ^{1}H to ^{31}P polarization transfer of HPO_4^{2-}. The extracted τ_{CP} and $T_{1\rho}$ were 0.39 ± 0.04 and 6.1 ± 0.5 ms, respectively.

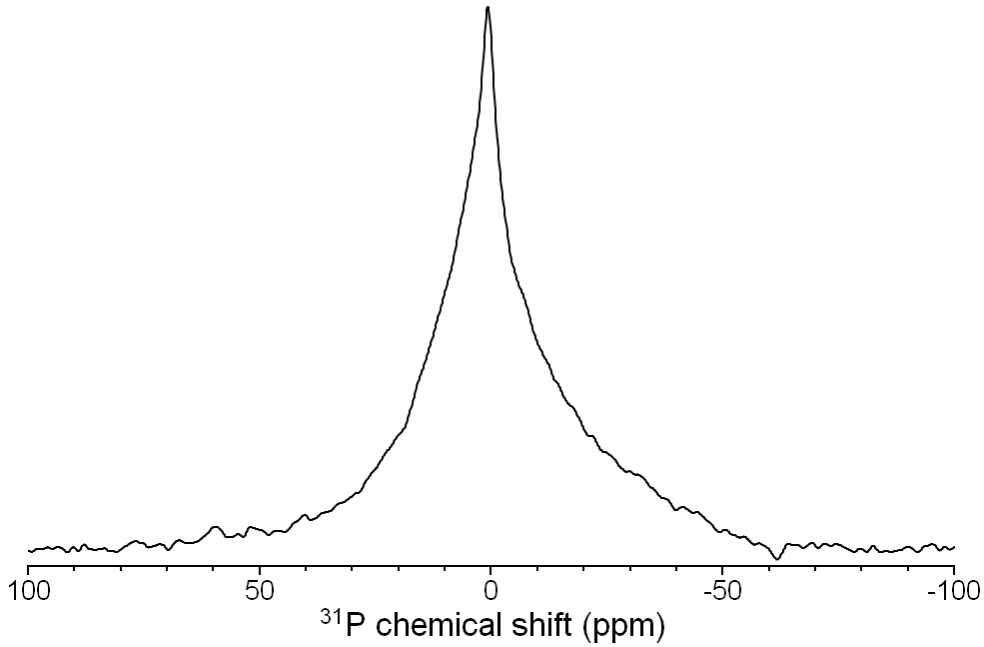

Figure S13. ^{31}P Bloch decay spectrum of the gel-like sample of CaP-PAA acquired under static conditions.

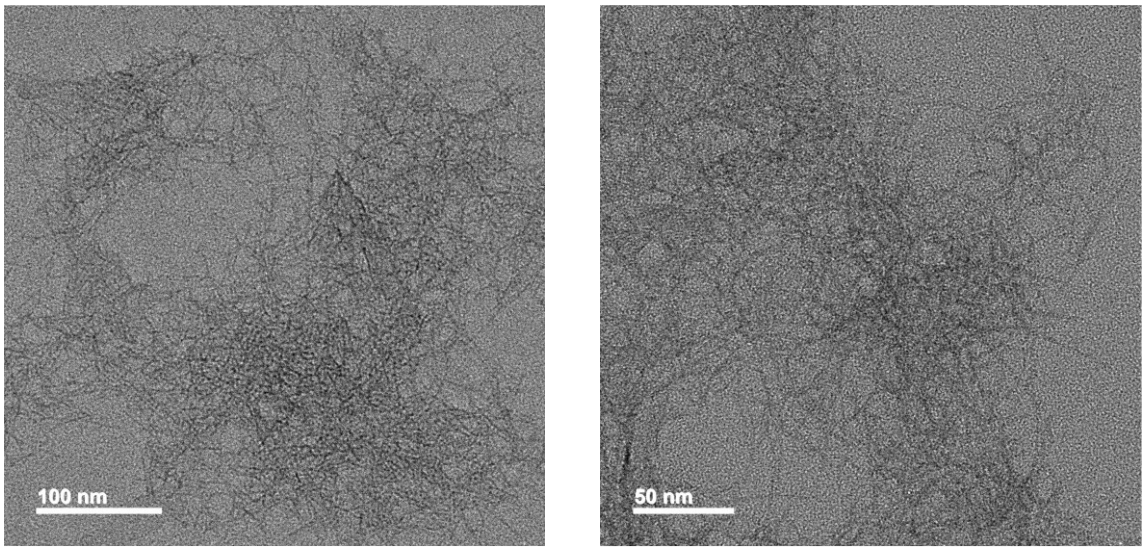

Figure S14. TEM images of the gel-like CaP-PAA resuspended in water.

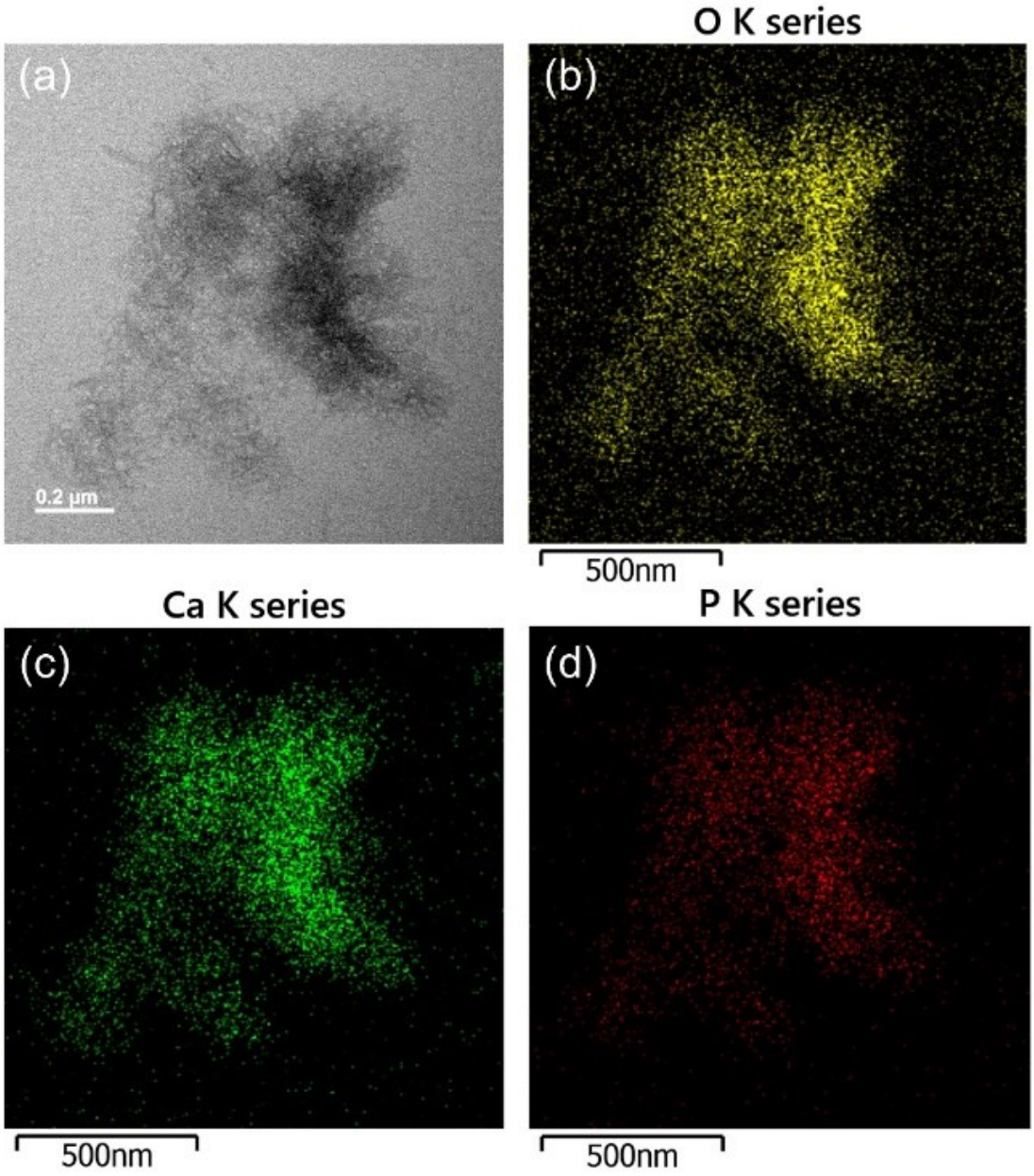

Figure S15. STEM image and EDX mapping of CaP-PAA: (a) STEM, EDX mapping of (b) oxygen, (c) calcium, and (d) phosphorus.

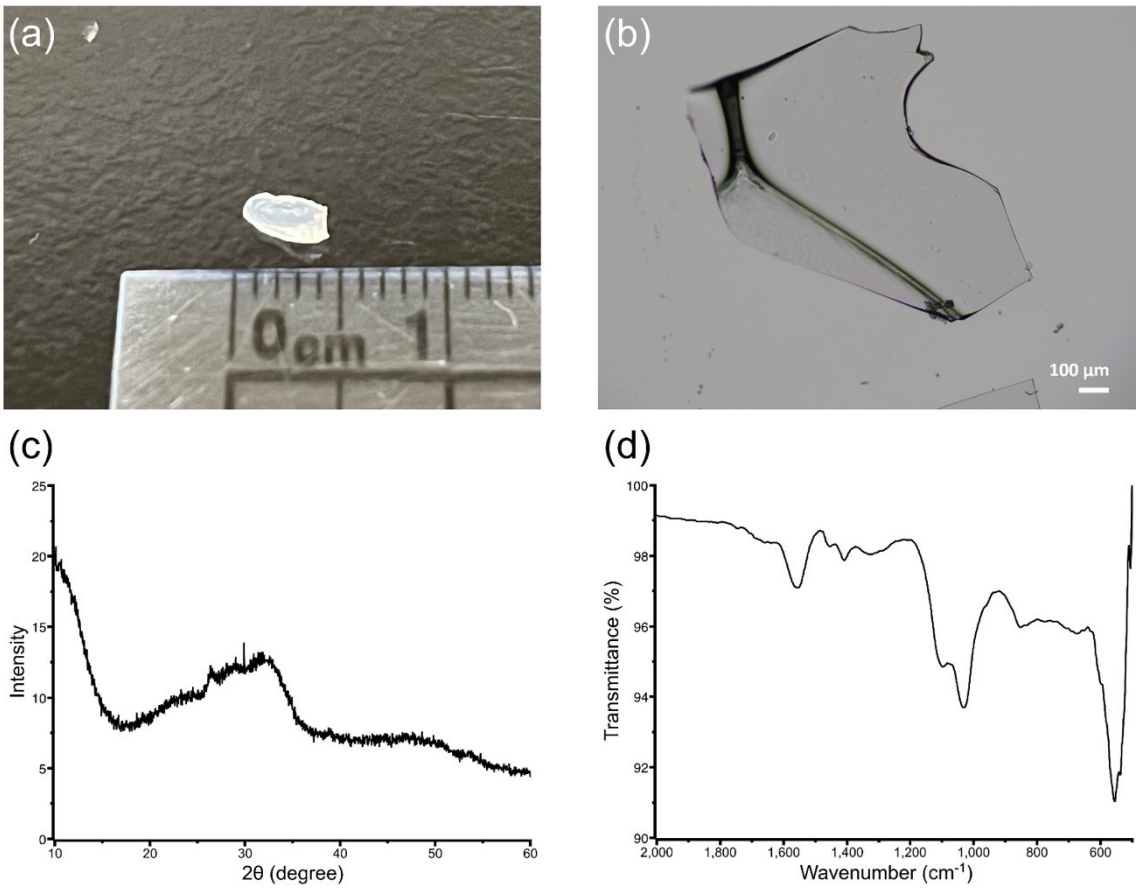

Figure S16. (a) Photo of the monolithic CaP-PAA after drying the gel-like precursor under reduced pressure for 48 h. (b) Optical image of the monolith sample of CaP-PAA. (c) XRD pattern of monolithic CaP-PAA. (d) FT-IR spectrum of monolithic CaP-PAA. As shown in (c) and (d), the sample was largely amorphous.

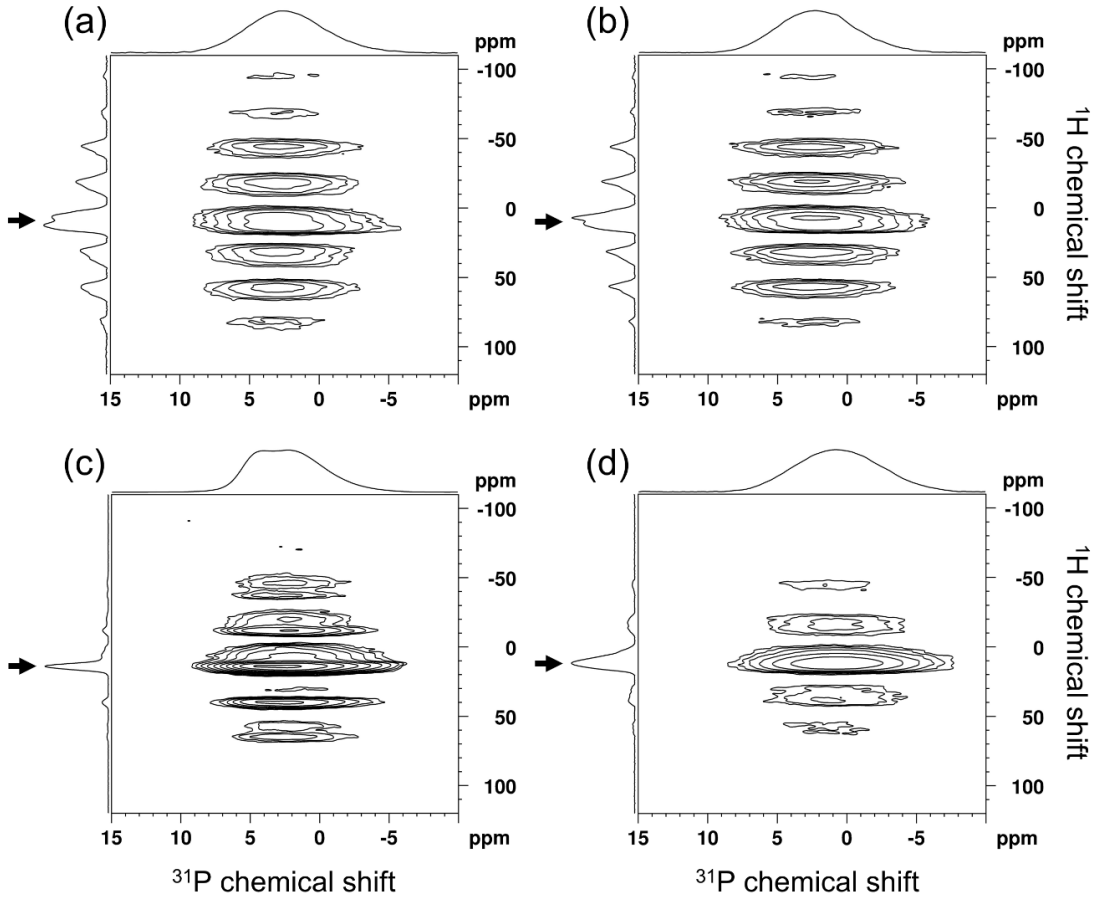

Figure S17. $^{31}P\{^{1}H\}$ HETCOR spectra shown with the full spectral window in the ^{1}H dimension: (a) ACP_{TEA} (monolith); (b) $ACP_{9.7}$; (c) CaP-PAA (monolith); (d) ACHP. The arrows indicate the center bands and other peaks are the spinning sidebands.

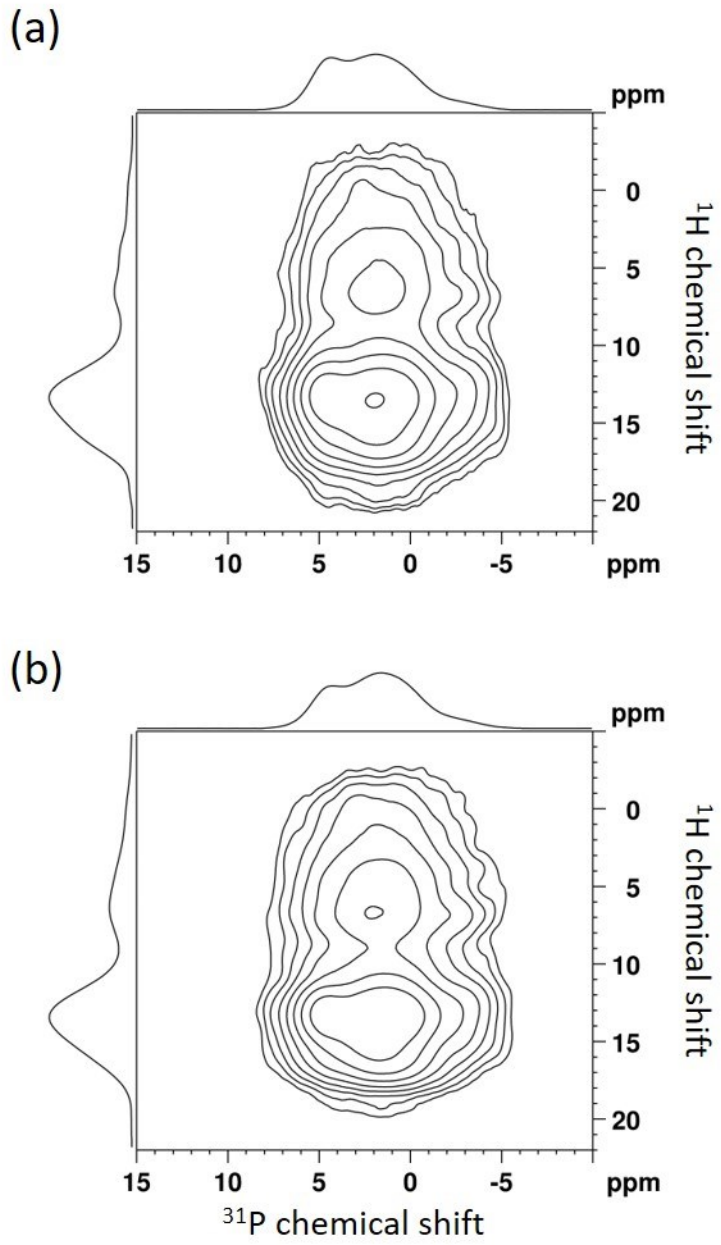

Figure S18. $^{31}P\{^{1}H\}$ HETCOR spectra acquired for CaP-PAA (monolith) at a contact time of 2 ms at spinning rates of (a) 10 and (b) 20 kHz. The contour levels were increased by a factor of 1.8 successively, where the base level was set to 5 × root-mean-square noise. There was no significant difference between two spectra.

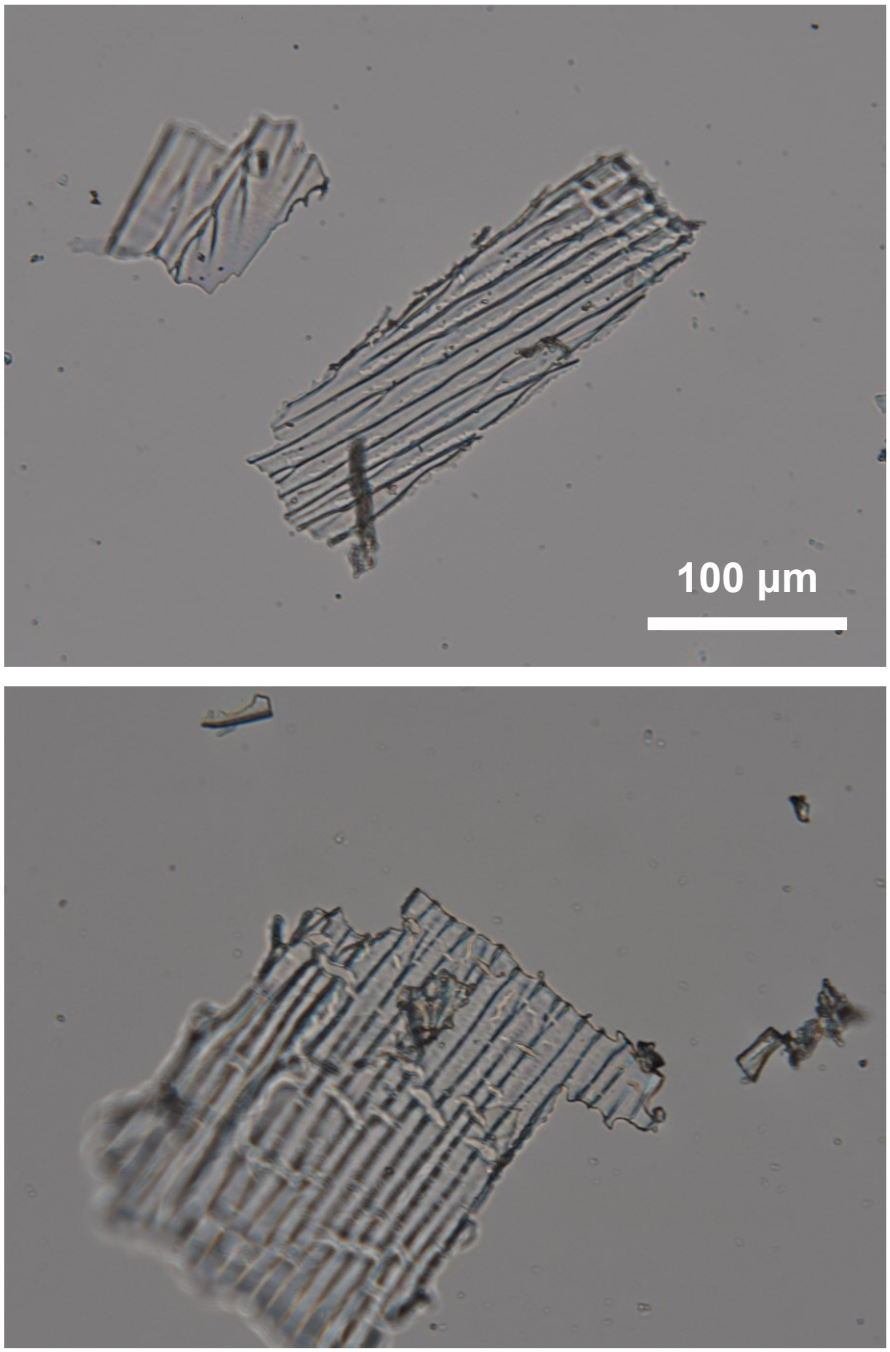

Figure S19. Optical images of CaP-PAA dehydrated by lyophilization for 24 hours. The parallel ridges were coined as "transition bars" (see the main text).

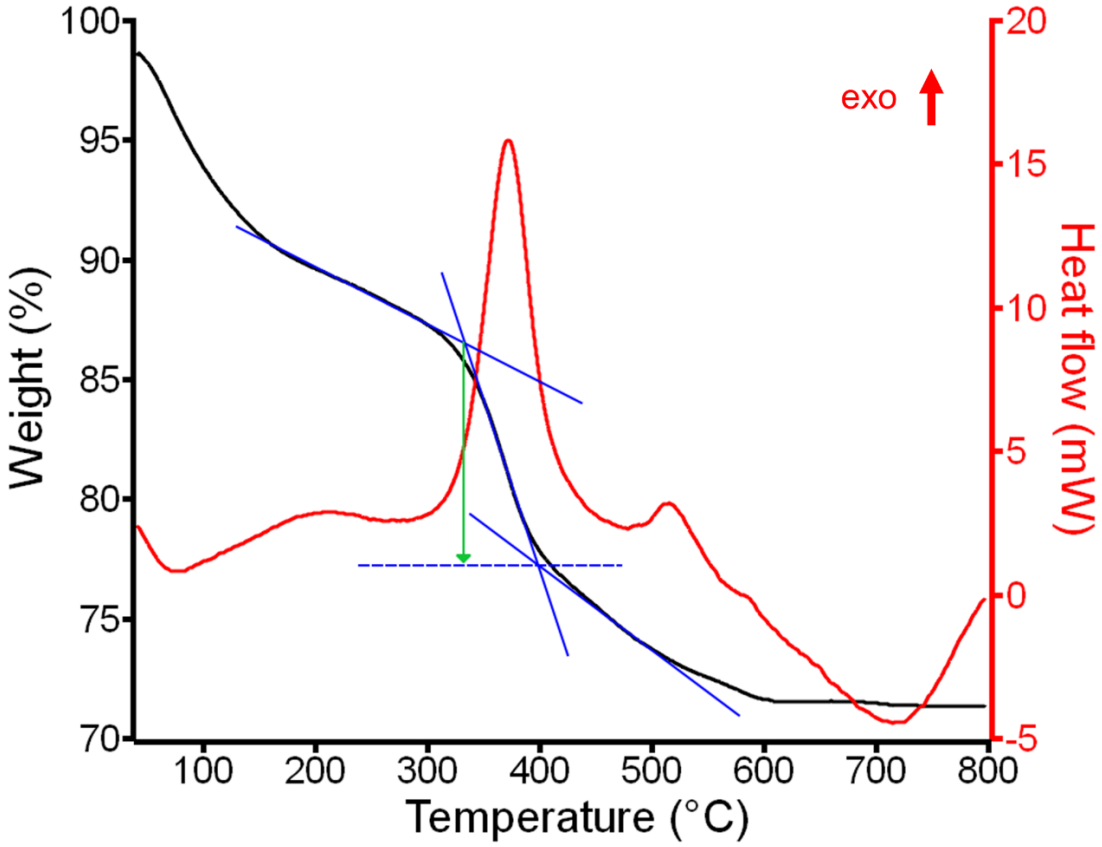

Figure S20. Thermogravimetric analysis (black) and differential scanning calorimetry (red) results of lyophilized CaP-PAA. The data were acquired in air at a heating rate of 10 °C/min. The weight loss due to PAA was estimated by the span of the arrow in green (9.2 wt%).

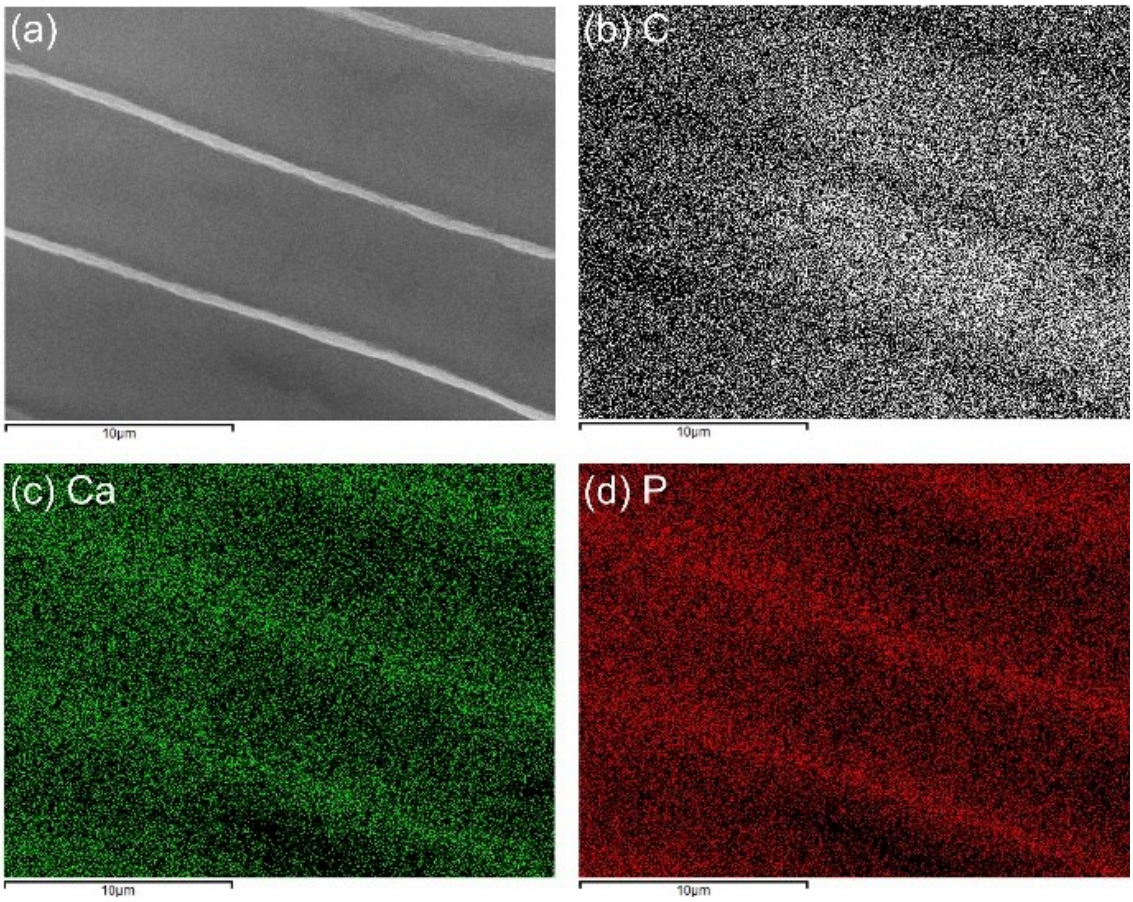

Figure S21. (a) SEM image of lyophilized CaP-PAA sample and the corresponding EDX mapping of (b) carbon; (c) calcium; and (d) phosphorus.

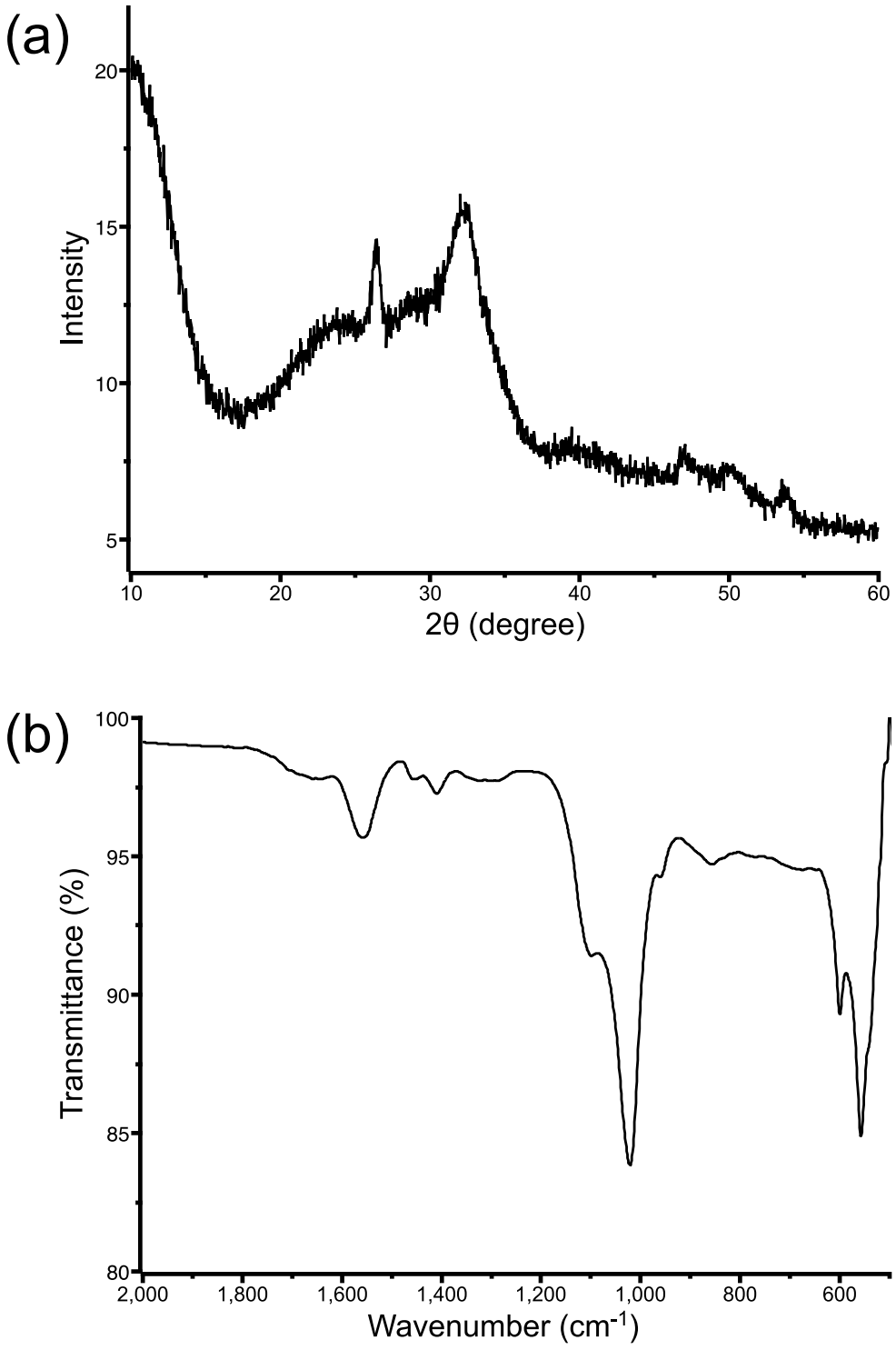

Figure S22. (a) XRD pattern and (b) FT-IR spectrum of lyophilized CaP-PAA.

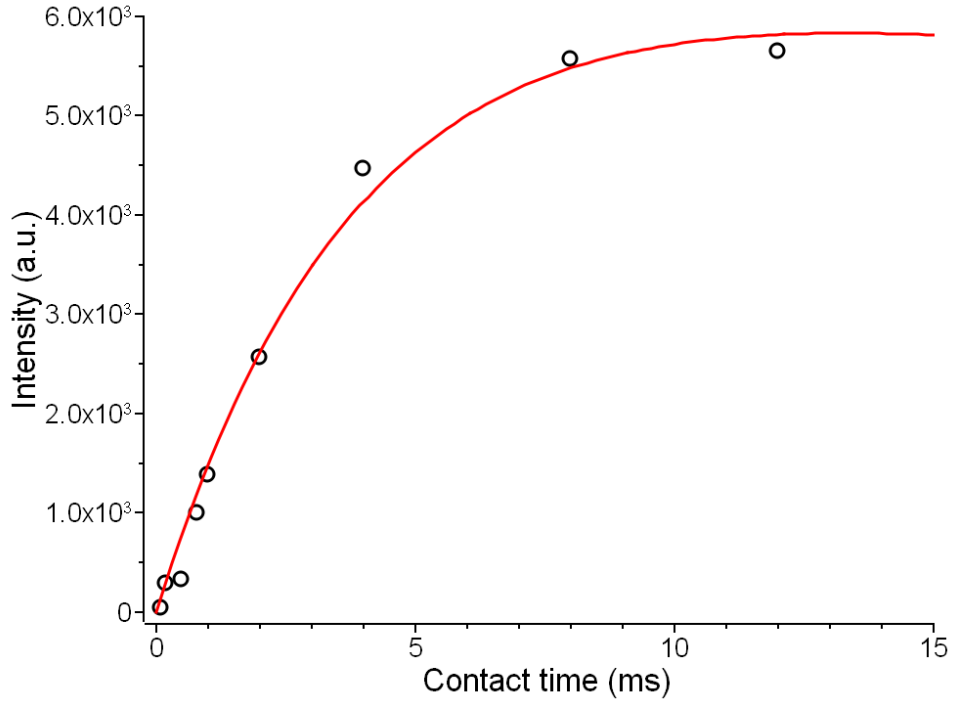

Figure S23. Fitting of the intensity modulation of the correlation peak at (^{1}H: 0.2 ppm, ^{31}P: 3.0 ppm) of the lyophilized CaP-PAA. The correlation peak corresponded to the ^{1}H to ^{31}P polarization transfer of OH^{-}/PO_4^{3-}. The extracted τ_{CP} was 4.1 ± 0.5 ms and $T_{1\rho}$ was set to be infinitely long.

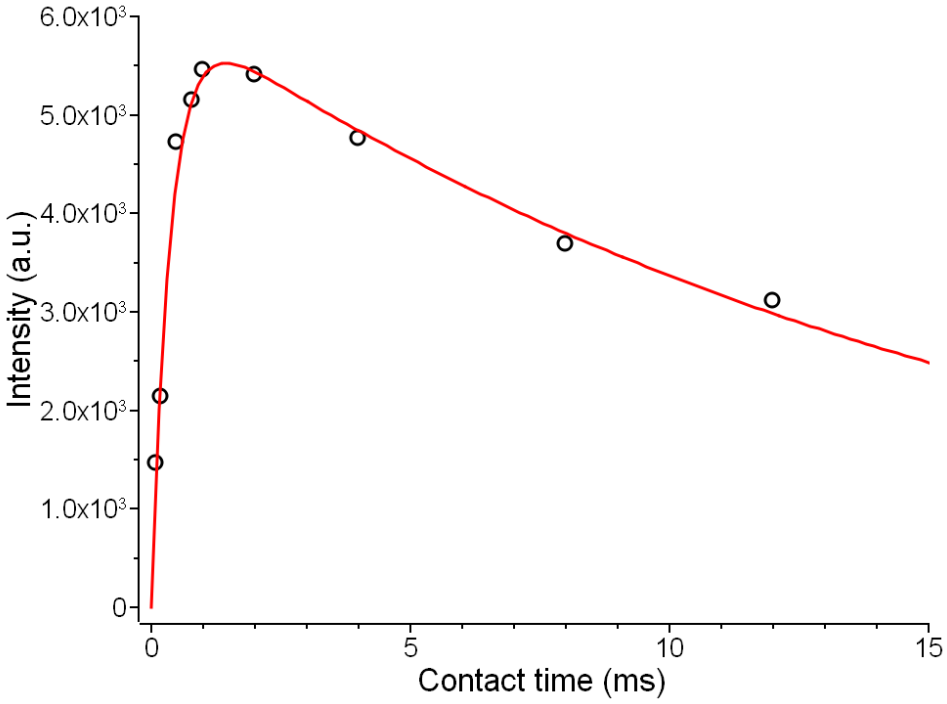

Figure S24. Fitting of the intensity modulation of the correlation peak at (^{1}H: 0.2 ppm, ^{31}P: 2.1 ppm) of the lyophilized CaP-PAA. The correlation peak corresponded to the ^{1}H to ^{31}P polarization transfer of OH^{-}/HPO_4^{2-}. The extracted τ_{CP} and $T_{1\rho}$ were 0.38 ± 0.04 and 16 ± 2 ms, respectively.

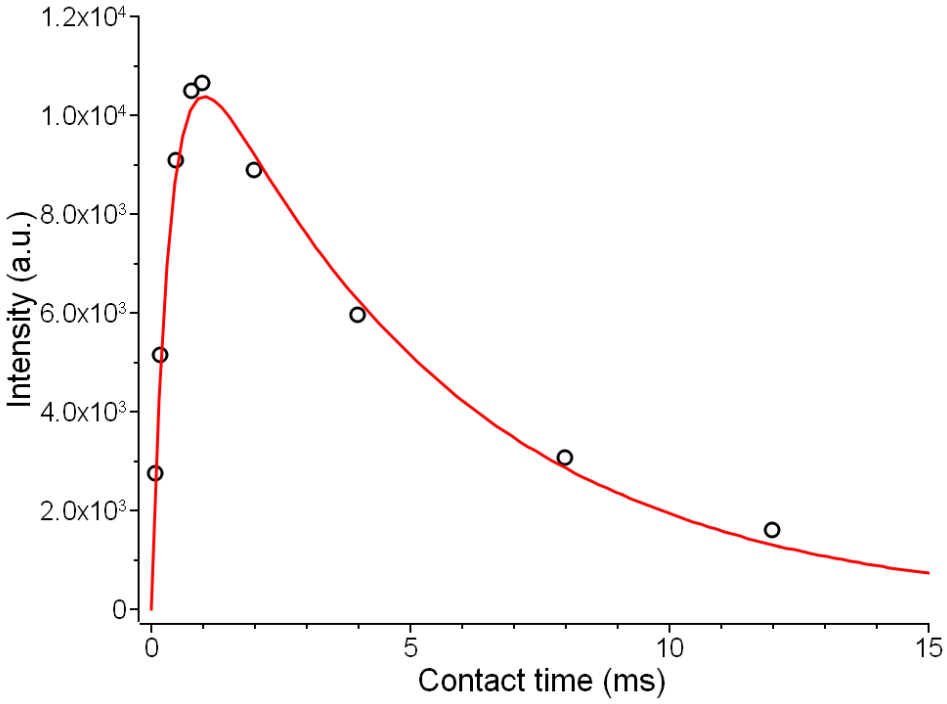

Figure S25. Fitting of the intensity modulation of the correlation peak at (^{1}H: 6.4 ppm, ^{31}P: 2.1 ppm) of the lyophilized CaP-PAA. The correlation peak corresponded to the ^{1}H to ^{31}P polarization transfer of H_2O/HPO_4^{2-}. The extracted τ_{CP} and $T_{1\rho}$ were 0.39 ± 0.03 and 5.1 ± 0.3 ms, respectively.

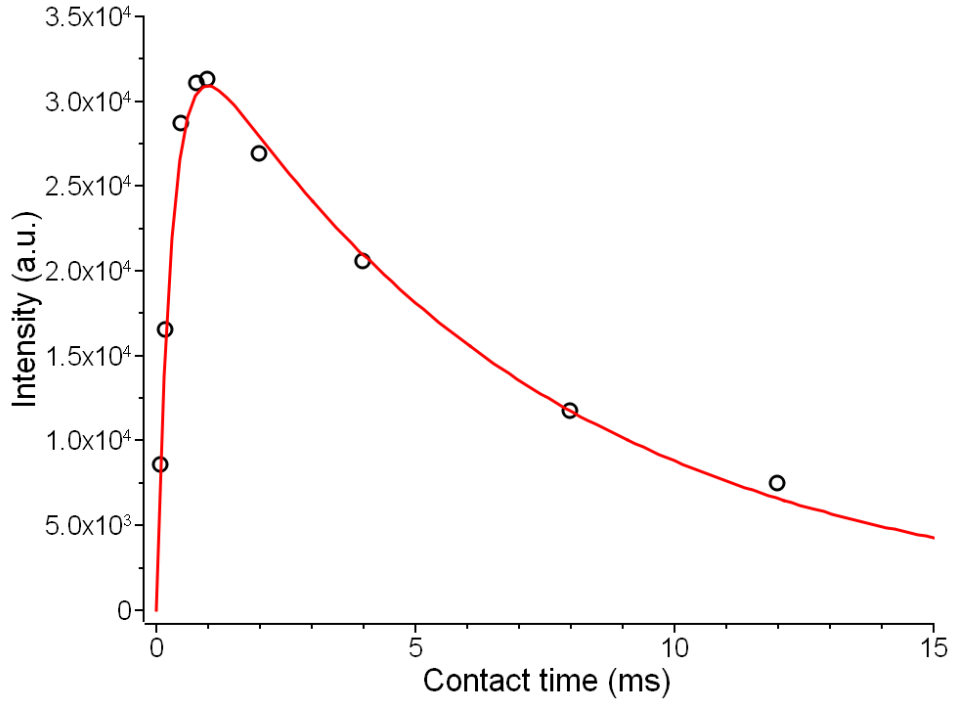

Figure S26. Fitting of the intensity modulation of the correlation peak at (^{1}H: 14.2 ppm, ^{31}P: 2.1 ppm) of the lyophilized CaP-PAA. The correlation peak corresponded to the ^{1}H to ^{31}P polarization transfer of HPO_4^{2-}. The extracted τ_{CP} and $T_{1\rho}$ were 0.32 ± 0.03 and 6.9 ± 0.5 ms, respectively.

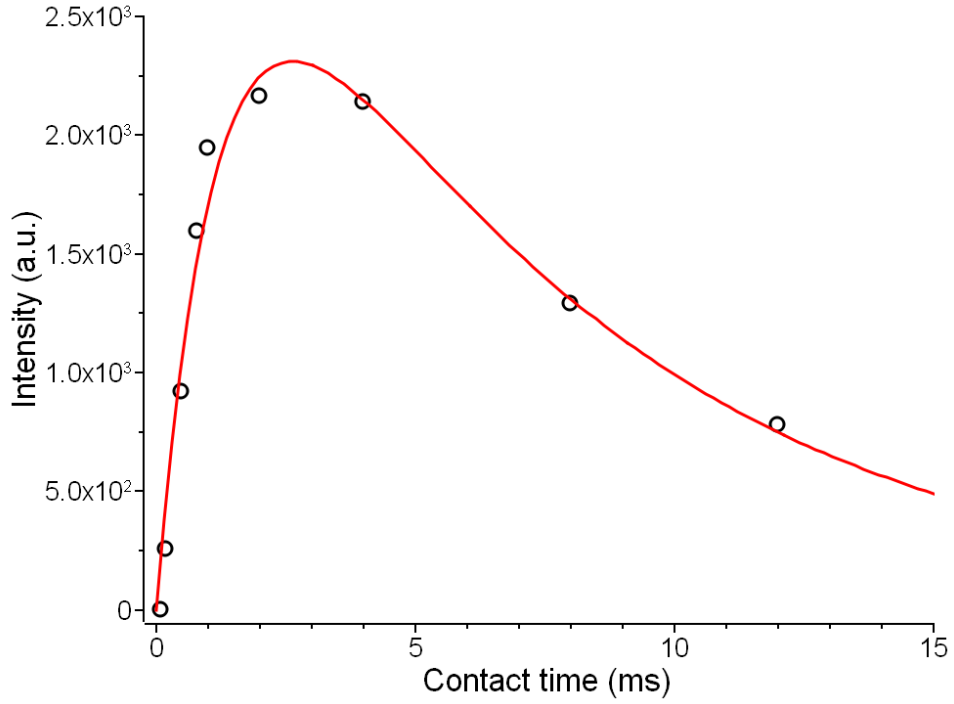

Figure S27. Fitting of the intensity modulation of the correlation peak at (^{1}H: 14.2 ppm, ^{31}P: 4.8 ppm) of the lyophilized CaP-PAA. The correlation peak corresponded to the ^{1}H to ^{31}P polarization transfer of HPO_4^{2-}/PO_4^{3-}. The extracted τ_{CP} and $T_{1\rho}$ were 1.52 ± 0.53 and 7 ± 2 ms, respectively.

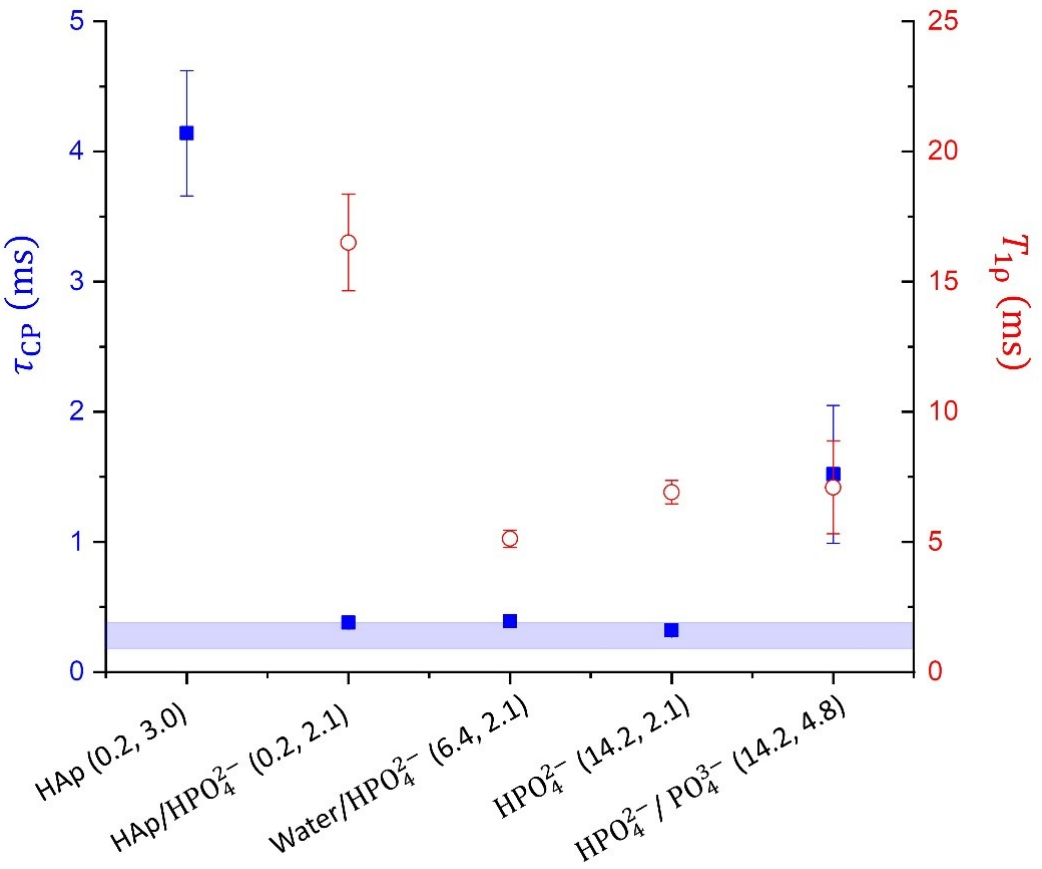

Figure S28. Summary of τ_{CP} and $T_{1\rho}$ of lyophilized CaP-PAA extracted from the fittings shown in **Figures S23–S27.** The shaded area indicates the τ_{CP} region corresponding to the ^{1}H to ^{31}P polarization transfer of HPO_4^{2-} for monetite.

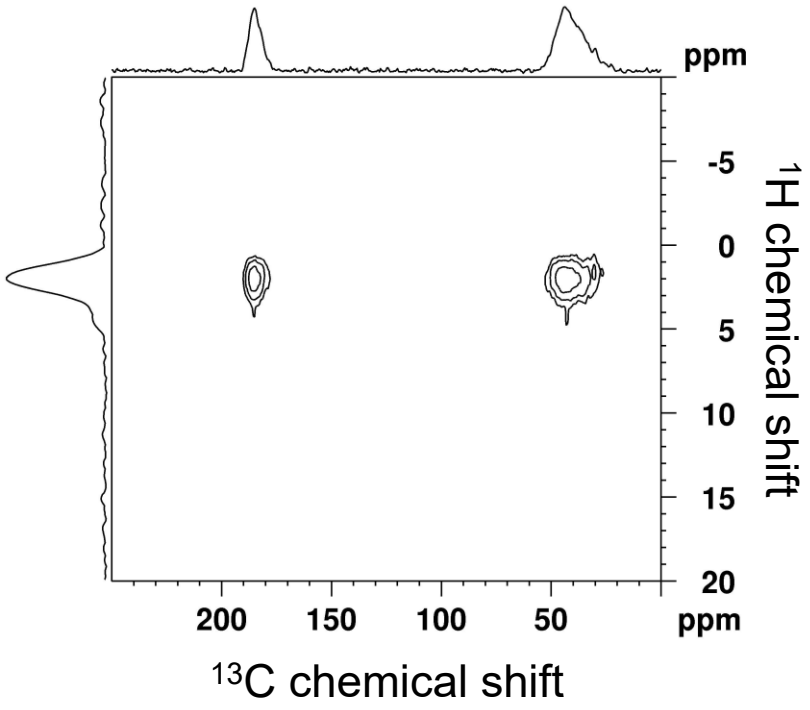

Figure S29. $^{13}C\{^{1}H\}$ FSLG-HETCOR spectrum acquired for lyophilized CaP-PAA at a contact time of 2 ms. The contour levels were increased by a factor of 1.8 successively, where the base level was set to 5 × root-mean-square noise. The ^{1}H peak at 2 ppm was assigned to the hydrogens of the alkyl chain of PAA.

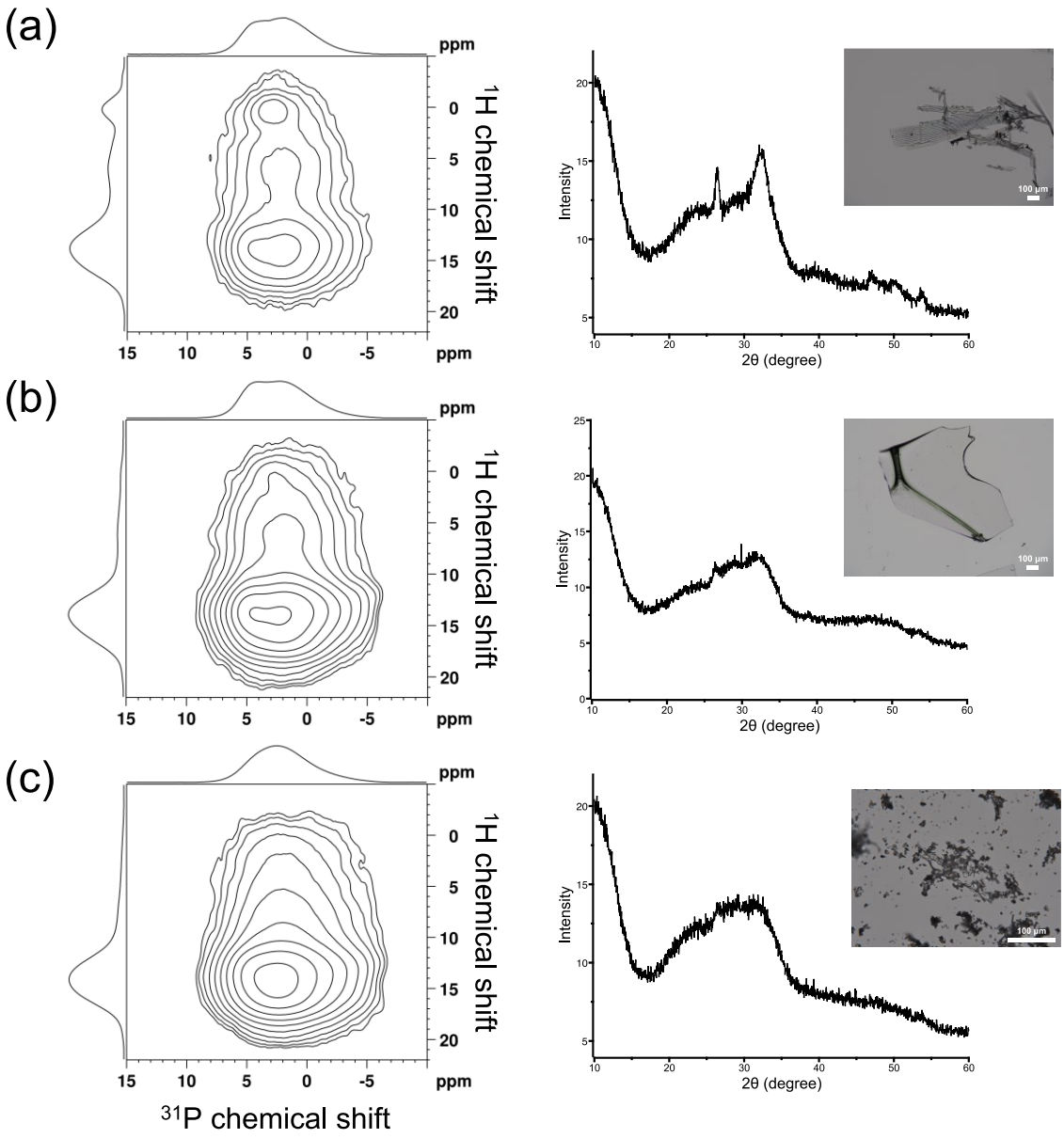

Figure S30. ^{31}P{^{1}H} HETCOR and FT-IR spectra of CaP-PAA dehydrated by (a) lyophilization; (b) drying under reduced pressure for 48 h; (c) drying in vacuo for 24 h. The figures on the right are the corresponding XRD patterns and the insets show the optical images of each sample.

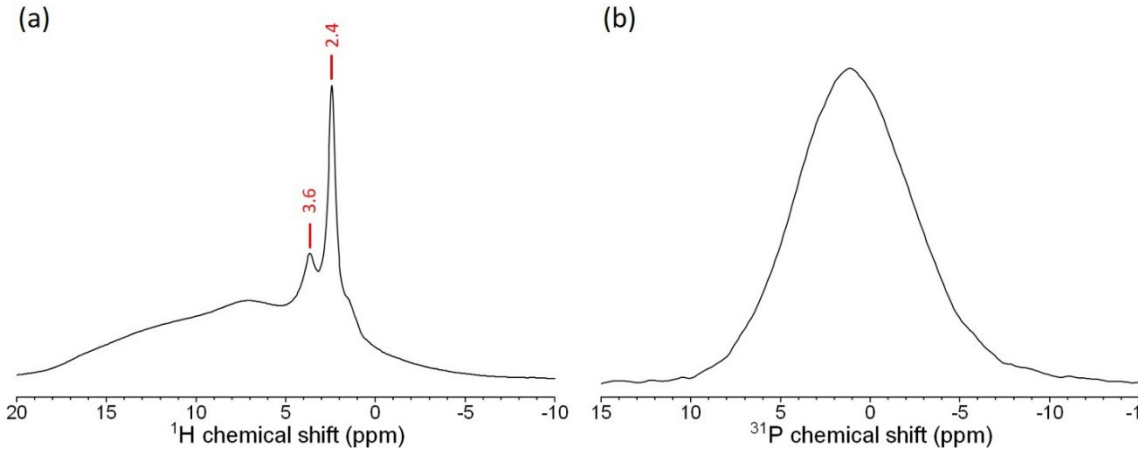

Figure S31. (a) ^{1}H and (b) ^{31}P MAS spectra (acquired by direct excitation) for ACHP were consistent with those reported in the literature.[4]

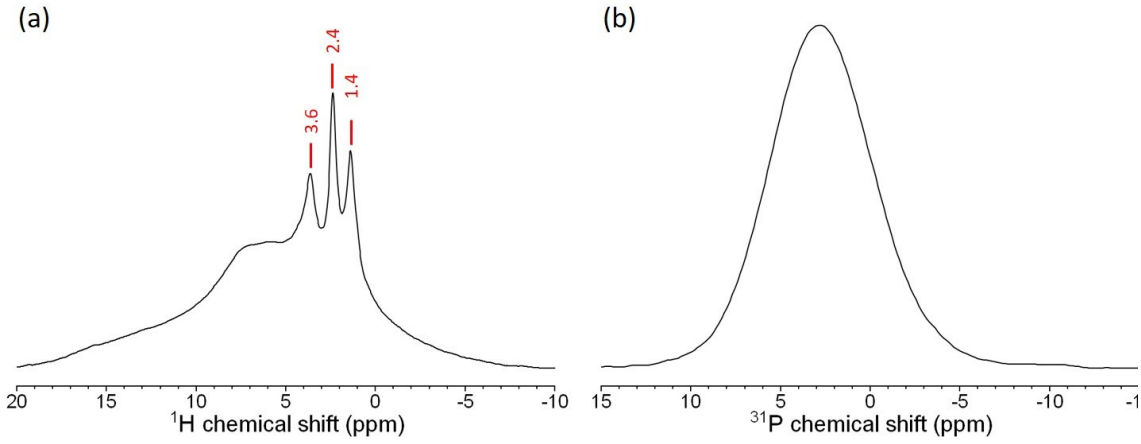

Figure S32. (a) ^{1}H and (b) ^{31}P MAS spectra acquired for $ACP_{9.7}$ were consistent with those reported for basic ACP.[4]

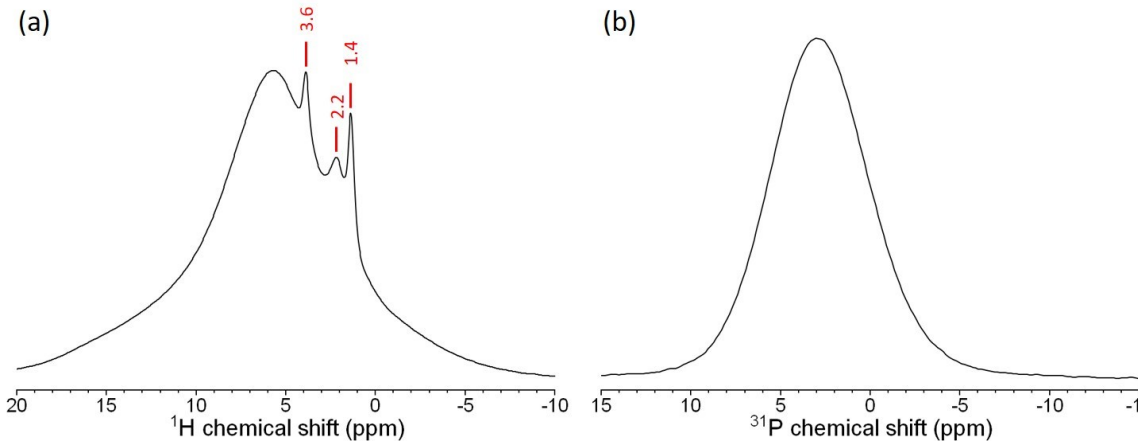

Figure S33. (a) ^{1}H and (b) ^{31}P MAS spectra of monolithic ACP_{TEA}.

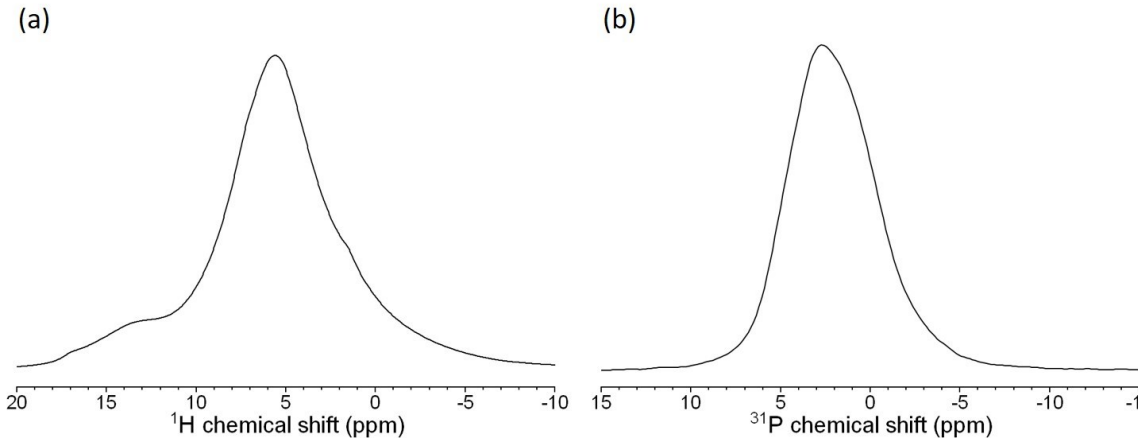

Figure S34. (a) ^{1}H and (b) ^{31}P MAS spectra of monolithic CaP-PAA. We do not fully understand why the ^{1}H MAS spectrum does not contain any sharp peaks as demonstrated in other ^{1}H MAS spectra of ACPs.

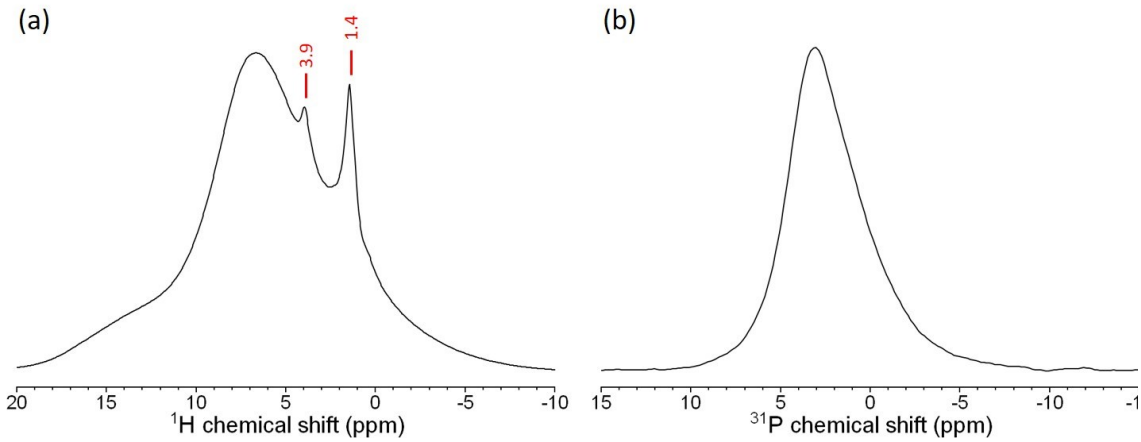

Figure S35. (a) ^{1}H and (b) ^{31}P MAS spectra of lyophilized CaP-PAA. The ^{1}H peaks at 3.9 and 1.4 ppm were tentatively assigned to the mobile water molecules physisorbed on the mineral surface.

4. Tables

Table S1. Summary of the NMR parameters extracted for the correlation peaks of the $^{31}P\{^{1}H\}$ HETCOR spectra of different samples.*

Sample	Assignment	^{1}H		^{31}P		M_0	τ_{CP} (ms)	$T_{1\rho}$ (ms)
		δ (ppm)	FWHM (ppm)	δ (ppm)	FWHM (ppm)			
ACHP	HPO_4^{2-}	13.2	6.9	0.7	7.2	--	0.38 ± 0.03	6.2 ± 0.4
$ACP_{9.7}$	H_2O/PO_4^{3-}	6.8	7.5	2.3	6.7	32380	0.97 ± 0.07	12 ± 1
	$H_2O \cdots HOPO_3^{2-}$	13.5	5.9	2.0	7.0	25660	0.56 ± 0.03	11.0 ± 0.5
Monetite	$H1P2O_4^{2-}$	16.3	1.4†	−0.4	1.4†	86530	0.20 ± 0.02	15 ± 2
	$H2P1O_4^{2-}$	13.5	3.0‡	−1.7	0.9†	98860	0.34 ± 0.04	31 ± 6
	$H2PO_4^{2-} \cdots HP2O_4^{2-}$	13.5	3.0‡	−0.4	1.4†	128750	0.42 ± 0.02	22 ± 1
	$H1PO_4^{2-}/HP1O_4^{2-}$	16.3	1.4†	−1.7	0.9†	51680	0.65 ± 0.03	44 ± 6
ACP_{TEA}	$HOH \cdots OPO_3^{3-}$	6.6	8.1	2.8	6.5	21660	0.47 ± 0.04	6.3 ± 0.4
	$H_2O \cdots HOPO_3^{2-}$	13.7	6.1	2.5	6.8	26360	0.39 ± 0.04	6.1 ± 0.5
CaP-PAA (Monolith)	$HOH \cdots OPO_3^{3-}$	6.1	6.3	2.0	5.0	12820	0.56 ± 0.04	9.3 ± 0.6
	HPO_4^{2-}	13.5	3.8	1.7	4.5	26960	0.35 ± 0.03	7.3 ± 0.5
	$HPO_4^{2-} \cdots PO_4^{3-}$	13.5	3.8	4.7	2.2†	12200	0.76 ± 0.07	8.0 ± 0.6
CaP-PAA (Lyophilized)	OH^-/PO_4^{3-}	0.2	2.2†	3.0	2.1†	6940	4.1 ± 0.5	n.d.
	OH^-/HPO_4^{2-}	0.2	2.2†	2.1	5.7	6170	0.38 ± 0.04	16 ± 2
	H_2O/HPO_4^{2-}	6.4	8.7	2.1	5.7	13670	0.39 ± 0.03	5.1 ± 0.3
	HPO_4^{2-}	14.2	4.9	2.1	5.7	37360	0.32 ± 0.03	6.9 ± 0.5
	HPO_4^{2-}/PO_4^{3-}	14.2	4.9	4.8	1.9†	4070	1.52 ± 0.53	7 ± 2

* The chemical shifts of the correlation peaks were obtained by the deconvolution of the ^{1}H and ^{31}P projections of the HETCOR spectra with contact time of 2 ms. The green and red colors

denote the source and the detected nuclei of the CP process. The species in close proximity are separated by "/", those with hydrogen bonding in between is connected by "…". † FWHM corresponding to crystalline phase. ‡There were two unresolved signals.

References

1 Z. Liu, C. Shao, B. Jin, Z. Zhang, Y. Zhao, X. Xu and R. Tang, *Nature*, 2019, 574, 394–398.

2 T. W. T. Tsai and J. C. C. Chan, in *Annual Reports on NMR Spectroscopy*, Elsevier, 2011, vol. 73, pp. 1–61.

3 Y. Yu, B. Stevensson, M. Pujari-Palmer, H. Guo, H. Engqvist and M. Edén, *Int. J. Mol. Sci.*, 2019, 20, E6356.

4 B.-Q. Lu, N. A. Garcia, D. M. Chevrier, P. Zhang, P. Raiteri, J. D. Gale and D. Gebauer, *Cryst. Growth Des.*, 2019, 19, 3030–3038.

Author Contributions

Shu-Li Li carried out all the NMR measurements and the deconvolution of the NMR spectra. Li-Han Wang prepared and characterized the samples. Yi-Tan Lin prepared the monolith of ACP following the Tang's protocol. Shing-Jong Huang assisted the NMR measurements. Jerry C. C. Chan supervised the experimental work and wrote the manuscript.